# Modeling of Fatigue Crack Growth in Composite Repair by Finite Element Method

Amit Shankar Kulkarni

A Dissertation Submitted to
Indian Institute of Technology Hyderabad
In Partial Fulfillment of the Requirements for
The Degree of Master of Technology


Department of Mechanical Engineering

June, 2011

# Declaration

I declare that this written submission represents my ideas in my own words, and where others' ideas or words have been included, I have adequately cited and referenced the original sources. I also declare that I have adhered to all principles of academic honesty and integrity and have not misrepresented or fabricated or falsified any idea/data/fact/source in my submission. I understand that any violation of the above will be a cause for disciplinary action by the Institute and can also evoke penal action from the sources that have thus not been properly cited, or from whom proper permission has not been taken when needed.

(Signature)

Amit Shankar Kulkarni
(Student Name)

ME09G002
(Roll Number)

# Approval Sheet

This thesis entitled "Modeling of Fatigue Crack Growth in Composite Repair by Finite Element Method" by Amit Shankar Kulkarni is approved for the degree of Master of Technology from IIT Hyderabad.

R. Prasanth Kumar 20/07/11

Dr. R. Prasanth Kumar, Asst. Professor, IIT Hyderabad
Examiner

B. Venkatesham 20/07/11

Dr. B. Venkatesham, Asst. Professor, IIT Hyderabad
Examiner

M. Ramji 20/07/11

Dr. M. Ramji, Asst. Professor, IIT Hyderabad
Adviser

Dr. B. Umashankar, Asst. Professor, IIT Hyderabad
Chairman

# Acknowledgements

I would like to express a deep sense of gratitude towards my guide Dr. M. Ramji for providing excellent guidance, encouragement and inspiration throughout the project work. Without his invaluable guidance, this work would never have been successful. I thank my parents for their constant support. I would like to thank Zencrack Ltd. for their technical support. I would like to thank PhD students Mrs. Shrilaxmi and Mr. Mohammad Kashfuddoja and my classmate Bhanu Prakash for helping and giving suggestions on modeling aspects. I would like to thank Mr. Srikanth who helped me in the software installation and licensing issues. I would like to thank Guruprasath sir for guiding and giving valuable suggestions regarding paper writing. Last but not least, I would like to thank the institute, mechanical engineering department, and head of the department. I would also like to thank all my classmates for their valuable suggestions and helpful discussions. Once again I would like to thank all the people who helped me directly or indirectly to successfully complete my work.

# Abstract

Fatigue failure is caused due to fluctuating loads and is one of the most common type of failure in mechanical structures. Fatigue damage starts with nucleation, crack formation and then propagation of the crack. Estimation of safe life of critical components becomes very essential in fail safe tolerant design for certification. Total life of a component generally consists of two stages viz. crack initiation and crack propagation. The proportion which each contributes will vary with the geometry, the loading and especially with the material.

Crack growth behaviour is a major issue in scheduling of inspection and maintenance in variety of industries especially in aircraft industry. Here, failure leads to catastrophic consequences and loss of life. When aircraft reach the end of their service life, fatigue cracks are found to have developed along rivet holes and other highly stressed regions of the aircraft. In order to extend the life of these aircraft, repairs are made to arrest these cracks. This is because huge financial costs involved in manufacturing of aircrafts. Hence, extending the life of in-service aircrafts can provide huge saving.

Life of these aircraft is extended by applying composite patches over the cracked panels. Composite patches provide an innovative repair technique, which can enhance the way aircraft are maintained. Instead of riveting multiple steel or aluminum plates to facilitate an aircraft repair, single composite doublers is bonded to the damaged structure. Adhesively bonded composite repairs also have many advantages over mechanically fastened repairs.

In this work, three-dimensional crack propagation study has been carried out for unrepaired and composite patch repaired panel using the finite element method. Analysis is done for the panel repaired with single side and double side patch considering the curved crack front. The panel is considered to be of Aluminum alloy 2024-T3 and boron/epoxy is the patch material. The numbers of cycles before failure are determined using Paris and Forman law. New patch material made of transversely graded material is proposed for a higher fatigue life.

# TABLE OF CONTENTS

# LIST OF TABLES

# LIST OF FIGURES

# Nomenclature

| | |
|---|---|
| SIF | Stress Intensity Factor |
| FEM | Finite Element Method |
| da | Incremental crack length |
| N | Number of cycles |
| $\vartheta$ | Crack inclination angle |
| Xc | X-Co-ordinate of Crack tip |
| Yc | Y-Co-ordinate of Crack tip |
| UCG | Uniform crack growth analysis |
| NUCG | Non uniform crack growth analysis |

# Chapter 1

# Introduction and Literature Review

## 1.1 Introduction

In real life applications, mechanical components are subjected to the several harsh fluctuating loads. This causes the fatigue failure of the components. It is impossible to avoid the fluctuating loads in practical applications. It has been observed that the most fracture failures are initiated by the fluctuating loads. Fatigue failure starts with initiation and then propagation of the crack.

Crack growth behaviour is a major issue in scheduling of inspection and maintenance in variety of industries. Aerospace structures and engines are an obvious example where failure leads to catastrophic consequences and loss of life. Numerous other examples can be cited in other engineering fields such pressure vessels, gas turbine engines, pipelines etc. The financial costs involved if an in-service component is found to contain a defect are a major factor in the search for numerical methods to predict 3D crack propagation. In addition, the ability to safely reduce maintenance intervals and extend the life of in-service components can provide huge saving.

Mere presence of a crack does not condemn a component or a structure to be unsafe and hence unreliable. Whether under cyclic or sustained loading, it is necessary to know how long an initial crack of certain size would take to grow to a critical size at which the component or structure becomes unsafe and fails. Also, by knowing how a crack evolves and its rate of propagation, one should be able to estimate the residual service life of a component under normal service loading conditions. Crack

propagation enables one to predict the period of sub-critical crack growth and hence the service life of a component.

Considering the case of aircrafts, when today's aircraft reach the end of their service life, fatigue cracks are found to have developed along rivet holes and other highly stressed regions of the aircraft. In order to extend the life of these aircraft, repairs have been made to arrest these cracks. Different repair methodologies available include applying metallic patches with riveted joints, applying adhesively bonded composite patches. In case of repair with mechanical fasteners, the panel and patch are mechanically fastened by using rivets. The major disadvantage of riveted joints is that there is a stress concentration at the rivet holes. It is difficult to detect the crack under the patch. Also, it has low patching efficiency. There exists a danger of corrosion under the patch.

Composite doublers or repair patches provide an innovative repair technique, which can enhance the way aircraft are maintained. Instead of riveting multiple steel or aluminum plates to facilitate an aircraft repair, single composite doublers is bonded to the damaged structure. Adhesively bonded composite repairs have many advantages over mechanically fastened repairs (Baker and Jones, 1988) [1] such as:

- no new stress concentration created by new rivet holes
- high stiffness-to-weight and strength-to-weight ratios of the patch, thus reducing drag
- patches are readily formed into complex shapes, permitting the repair of irregular components;
- high fatigue and corrosion resistance of the composite
- potential time savings in installation.

This repair technique has been primarily used in the area of military aviation. The composite patches thus result in enhancing life span of the component.

In this study, fatigue crack growth modeling is done using finite element methods applied to both unrepaired and repaired panel. At first two dimensional analysis carried out to correctly predict crack growth. Later, a detailed three dimensional analysis is carried out. The same approach is then carried out for fatigue crack growth analysis of repaired panels.

## 1.2 Literature Review

Composite patch repair is most widely used for repairing of aircrafts. The main objective of patch repair is to extend life of flawed components at reasonable cost. Main objective is fatigue enhancement, crack patching or corrosion repair. There are two types of composite repairs, namely single side and double side patch repair. In case of single sided patch, the composite patch is applied only on one side whereas in double sided patch, patches are applied on both sides as shown in Fig. 1.1.Single sided repair is often called as unsymmetrical repair since the structure becomes unsymmetrical. The double sided repair is referred to as symmetrical repair.

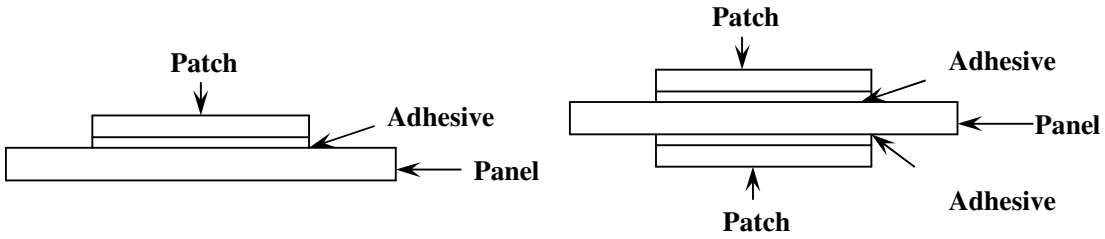


**Figure 1.1:** Schematic of (a) Single side patch repair (b) Double side patch repair


**Figure 1.2:** Application of patch repair to the wing of F-111 military aircraft [1]

Figure 1.2 shows one of the typical applications of composite patch repair carried out on the wings of military aircraft. It shows the single side patch on the lower side of the wings of F-111 military aircraft. The use of adhesively bonded repairs was initiated in 1970s by Baker and his coworkers. In 1978, patching in military aircrafts utilizing boron fiber reinforced plastics are described which prevent or considerably reduce crack propagation due to fatigue in cracked aircraft component. Baker and Jones [1] studied a repair technique using adhesively bonded boron/epoxy composite patches which became cost effective and most reliable. Also it has gained considerable popularity in the last two decades.

One of the most challenging aspects of bonded composite repair technology has been the stress analysis of repaired panels and the estimation of subsequent fracture parameters. The difficulty arises from the fact that a thin metallic panel under the in-plane loading would develop highly complicated three-dimensional stresses, if composite patches are bonded to its surface asymmetrical (single-sided repair). In many studies, the variation of stresses over the thickness of the cracked plate has not been investigated [1–5]. The stress variations over the thickness of a cracked plate in un-symmetric repair present a greater challenge in modeling due to the existence of out-of-plane bending. Hosseini-Toudeshky et al. [5] have studied the fatigue life assessment of repaired panels with adhesively bounded composite plates subjected to mode-I loading.

The previous investigations on fracture analysis of repaired aluminium panels using composite patches are mainly restricted for cracked components in mode-I condition. There are only few works available in literature on repaired panels having mixed-mode conditions [6, 7].

These works do not investigate the fatigue crack growth life and crack propagation direction of the repaired panels in mixed-mode condition using numerical approaches. Bachir Bouiadjra et al. [6] studied the computation of the stress intensity factors for repaired cracks with bonded composite patch in mode-I and mixed mode condition under static load case.

Chung and Yang studied the mixed-mode fatigue crack growth in aluminium plates with composite patches [7]. They performed experimental studies on crack growth behaviour and crack growth rate of panel repaired with single side patch.

Hosseini-Toudeshky et al. [8] studied the mixed mode fracture analysis of aluminium repaired panels using single side patches. They evaluated the fatigue

crack growth for unrepaired and composite patch repaired specimens. They also studied the effect of patch layer orientations on the crack growth rate and crack propagation direction. He considered the uniform crack growth in this study i.e. crack front line remains perpendicular to the plate surface as it grows.

Hosseini-Toudeshky [9] also experimentally examined the effects of composite patches on fatigue crack propagation of single-side repaired aluminum panels under mode-I condition. The author has studied the effect of variation of crack growth life with panel thickness. Both uniform crack growth analyses (UCG) and non-uniform crack growth analysis (NUCG) has been modeled in that work. Figure 1.3 shows UCG and NUCG crack front shapes. It is seen that the lives obtained with non-uniform crack growth analysis are close to those obtained from experiments.

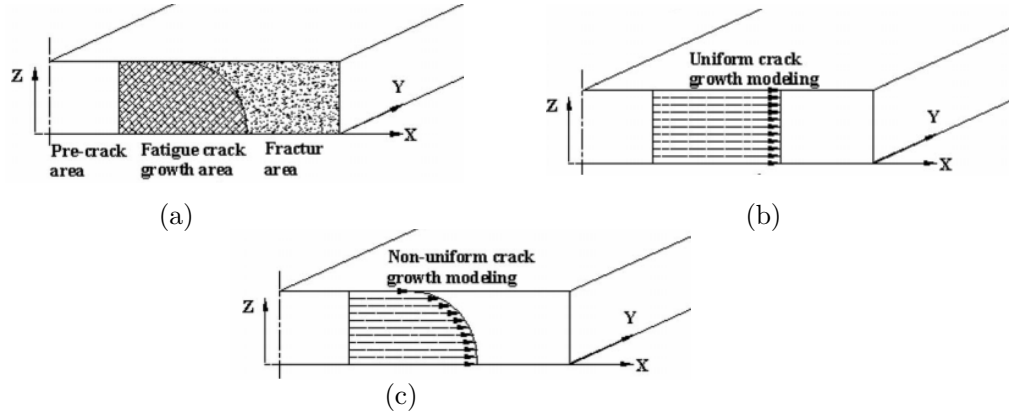


**Fig. 1.3:** Crack front shape during its propagation after the repair (a) Real fracture surface (b) Crack front at UCG (c) Crack front at NUCG [9]

Whereas, the lives calculated using the mid-plane results in uniform crack growth analyses (UCG) are non-conservative by the order of 35–90% comparing with the experimental results. Hosseini-Toudeshky and Mohammadi [10] studied the simple method to calculate the crack growth life of adhesively repaired aluminium panels under mode-I condition. In this study they evaluated the crack growth life of the repaired panels using uniform and non-uniform crack growth model. Hosseini-Toudeshky et al. [11] studied crack propagation of adhesively bonded repaired panels in general mixed-mode conditions using the finite element method. In this study they have studied mixed mode conditions of single sided patch with non-uniform crack growth. They have used Paris law for the life estimation.

There are very few papers which have considered curved crack front while performing crack growth analysis. In this work, the crack growth analyses has been

carried out for mode-I and mixed-mode conditions considering a curved crack front i.e. non uniform crack growth. Analysis is done for unrepaired panel, panel repaired with single and double side patches having various crack inclination angles. The fatigue life is estimated using Paris and Forman law. Effect of transversely graded patch on the fatigue life improvement has also been studied in this work.

## 1.3 Scope and Motivation

Fatigue modeling of composite repaired panel is a relatively new area and the behavior of it is very complex as many parameters are involved. The non-uniform fatigue crack growth modeling becomes critical as it is in line with the experimental behaviour. Not much understanding is available in the literature on the modeling aspect of it. Also most of work present till date is applied for mode-I loading and most of the practically occurring problems are of mixed mode loading. There exists a scope for three dimensional modeling of fatigue crack growth behavior in repaired panels. Also the need for doing repetitive and time consuming experiments can be replaced by accurate modeling considering all the important parameters. Further, there is scope for trying new patch materials such as graded composites for a better performance.

## 1.4 Thesis Layout

Chapter 1 mainly consists of the introduction to the crack propagation, literature review, scope and objective of the project.

Chapter 2 considers the two dimensional analysis of the edge crack specimens for different crack inclination angles. This chapter discusses about the fracture and fatigue analysis of two dimensional edge crack specimens. It also discusses the three dimensional analysis of unrepaired panel. It consists of the overall methodology of three dimensional analysis.

Chapter 3 consists of the analysis of panel repaired with composite patch. This chapter discusses about the single side, double side and transversely graded patch repair.

Chapter 4 deals with the future work and recommendations.

# Chapter 2

# Fatigue Crack Propagation Modeling of Unrepaired Panels

## 2.1 Introduction

Fatigue failure is caused due to fluctuating loads. It starts with nucleation and then propagation of the crack. Total life of a component generally consists of two stages viz. crack initiation and crack propagation. The proportion which each contributes will vary with the geometry, the loading and especially with the material. In this work, only crack propagation life has been considered.

In general, for design of particular component three design philosophies are used viz. safe-life, fail-safe, damage-tolerant design. In the safe-life philosophy products are designed to survive a specific design life with a chosen reserve. Calculation alone may be used, or there may be some testing. The design life will then be some fraction of the estimated life. In general, this philosophy results in somewhat optimised structures. The penalty is that components have to be taken out of service when it is likely that they still have substantial remaining life. Furthermore, with the approach there is always a possibility that components will be very reliable and over designed. To reduce some of this waste of useful fatigue life, and maintain or improve the operating safety of a component in the later stages of its life, the philosophy of fail-safe may be adopted. An inspection procedure to detect the failure is needed, and a clear definition of action to be taken following this inspection must be specified. In case of damage-tolerant design, a more subtle inspection criterion is to inspect all components periodically to see whether or not cracks have started. If a crack is found the component could be taken out of service

immediately, but it is possible that failure is not imminent. We would then need information about the loading, how that loading affected crack growth and how big a crack would be needed to cause collapse. This is the basis of Damage-Tolerant design. It needs a close understanding of how cracks grow steadily under varying load and extend catastrophically when they reach a certain length. When using this approach, a clearly defined inspection procedure and agreed action following the result of this inspection is required.

The concept of studying crack propagation comes under damage-tolerant design philosophy. The most important application of crack propagation study is in aircrafts. Whenever crack is found on the wings of aircraft, the composite patch is applied to it to extend its service life. The reason for studying crack propagation is due to the huge financial costs involved in manufacturing of aircrafts. Hence, with this approach, we can use that aircraft for some more time.

The crack propagation study can be done experimentally as well as numerically i.e. by FEM. The experimental analysis is very much time consuming and costly. Sometimes, it is not possible to carry out analysis for particular cases experimentally. On the other hand, numerically, we can simulate it with less time and cost for different conditions.

In this chapter, crack propagation analysis has been carried out for unrepaired panels. Initially, two-dimensional analysis for was carried out and then in later stage, three-dimensional analysis was carried using FEM.

## 2.2 Fracture analysis of Two-Dimensional Models

In this section fracture analysis of two-dimensional models has been considered. The analysis has been carried out for mode I and mixed mode problems. Firstly, *J*-integral is evaluated from FEM. Then, from that stress intensity factors $K_{\mathrm{I}}$ and $K_{\mathrm{II}}$ are calculated from it. The details about the procedure and specimens have been discussed in further sections.

### 2.2.1 Two-Dimensional Model

Initially to start with, 2D analysis of unrepaired panel having edge crack was carried out. The meshing around the crack tip is very important aspect while studying crack propagation using FEM. Fine meshing is required around the crack

tip. The meshing for 2D models is relatively simpler than meshing required for 3D models. Hence, initially to start with, 2D models were considered for carrying out crack propagation analysis. Then, analysis was carried out for 3D models of unrepaired panel and composite patch repaired models.

#### 2.2.1.1 Straight Edge Crack Model

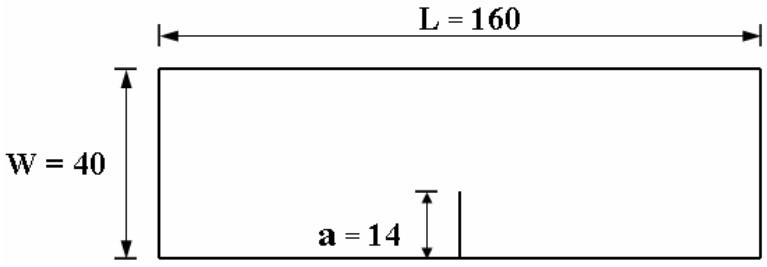


**Figure 2.1:** Dimensions of Straight Edge Crack Plate (All dimensions are in mm)

The Fig. 2.1 shows the typical geometry of the single edge crack model having a straight crack. Its length is 160 mm, width is 40 mm and thickness '$t$' is 12 mm. The crack length '$a$' is 14 mm. The material used is aluminium alloy 2024-T3. This material is mostly widely used as aircraft structures. Its Young's modulus ($E$) is 71.02 GPa and Poisson's ratio ($\nu$) is 0.3. These properties are taken from Ref. [8]. As the model is of mode-I, the crack front will propagate in a straight line. Having obtained the stress and strain fields around the crack tip using finite element, fracture parameters such as the stress intensity factor (SIF) denoted as $K_{\mathrm{I}}$ is estimated. Further, using an appropriate fatigue law the panel life is determined. For simplicity, linear elastic fracture mechanics (LEFM) behaviour has been assumed during crack growth analysis. For the determination of SIF, $J$-integral value is estimated. The $J$-integral definition [12, 13] considers a balance of mechanical energy for a translation in front of the crack along the x-axis, which is a path independent contour integral defined as

$$\oint_c [W n_1 - \sigma_{ij} n_j \frac{\partial u_i}{\partial x}] ds \tag{1}$$

where $W$ is strain-energy density; $\sigma_{ij}$ are stress elements; $u_i$ are the displacements corresponding to local $i$ -axis; s is the arc length of the contour; $n_j$ is the $j^{\text{th}}$

component of the unit vector outward normal to the contour $C$, which is any path of vanishing radius surrounding the crack-tip.

The $J$-integral value is directly obtained from Ansys which uses domain integral method for computation [5]. Using the assumption of linear elastic fracture mechanics and from Eq. (2), the $K_I$ parameter is related to the $J$-integral value as shown in Eq. (2) [12, 13]:

$$J = K_I^2 / E' \tag{2}$$

where $E'$ is the modulus of elasticity, $E' = E$ for plane stress condition, and is $E' = E/(1-\nu^2)$ for plane strain conditions. Hence, from Eq. (2) one can get the value of $K_I$ for various crack-tip positions as the crack grows. The analytical expression for the stress intensity factor for an edge crack specimen is given below [13]:

$$K = \sigma\sqrt{(\pi a)} * f(a/w) \tag{3.1}$$

$$f(a/w) = 1.12 - 0.23*\alpha + 10.55*\alpha^2 - 21.72*\alpha^3 + 30.39*\alpha^4 \tag{3.2}$$

where $\alpha = a / w$. The estimated SIF from finite element method will be compared against the SIF obtained using Eq. (3) for the model validation.

#### 2.2.1.2 Inclined Edge Crack Model

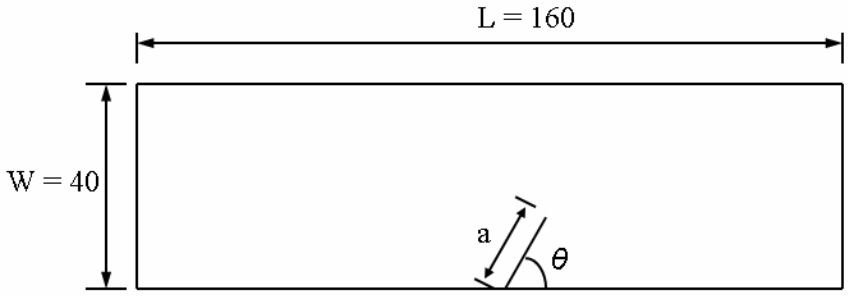


**Figure 2.2:** Dimensions of Inclined Edge Crack Plate (All dimensions are in mm)

Fig. 2.2 shows the geometry of the inclined edge crack model in mixed mode conditions. In this paper the analysis is done for the 30°, 45° and 60° crack inclination angles. As the crack plane is inclined with respect to the load, it becomes a mixed mode problem. Therefore one has to obtain both $K_I$ and $K_{II}$ for

characterizing the stress field around crack tip. Also, the fatigue life is determined using modified crack growth law incorporating both these SIF into it. Using the assumptions of linear elastic fracture mechanics and following Eq. (4), $K_I$ and $K_{II}$ are related to the $J$-integral as shown below [8]:

$$J = K_I^2 / E' + K_{II}^2 / E' \tag{4}$$

where $E'$ is the modulus of elasticity, $E' = E$ for plane stress condition, and is $E' = E/(1-\nu^2)$ for plane strain conditions. To solve the problem for determining $K_I$ and $K_{II}$, the ratio of $K_I$ over $K_{II}$ is obtained from the ratio of the normal distance to the horizontal distance of two closest nodes to the crack-tip which they have been coincided before loading as shown in Fig. 2.3. This procedure has been taken from Ref. [8].

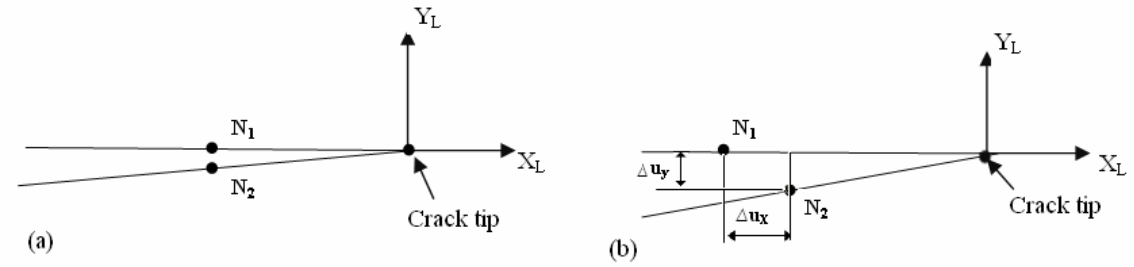


**Figure 2.3:** (a) Two coincident nodes near the crack tip before loading and (b) Two nearest nodes near the crack tip after loading.

Several criteria have been proposed to predict crack propagation direction in mixed-mode fracture problems. The major criteria presented so far to find a crack propagation direction are: stress-based criteria, energy-based criteria, and strain-based criteria. The most commonly used criteria are those based on the stress and energy. Previous research work shows that there are no significant differences between the obtained crack trajectories based on various crack propagation criteria [8].

The maximum tangential stress (MTS) criteria is the first criterion presented by Erdogan and Sih [12, 13]. This criterion states that a crack propagates in a direction corresponding to the direction of maximum tangential stress along a constant radius around the crack-tip. The MTS-criterion is based on the assumption that the material behaves ideally brittle. Using the Westergaard's stress field in the

polar coordinates and applying the MTS-criterion, the following equation is obtained as shown below [8]:

$$\tan^2\left(\frac{\alpha}{2}\right)-\frac{\mu}{2}\tan\left(\frac{\alpha}{2}\right)-\frac{1}{2}=0 \tag{5}$$

where $\mu$ is defined as the ratio of $K_{\mathrm{I}}$ over $K_{\mathrm{II}}$ ($\mu = K_{\mathrm{I}} / K_{\mathrm{II}}$) and $a$ is incremental crack propagation angle. To find the maximum root value of Eq. (5), the condition of $\partial^2\sigma_\alpha / \partial\alpha^2 < 0$ needs to be satisfied which leads to the following Eq. (6) [8]:

$$-\frac{3}{2}\left[\left(\frac{1}{2}\cos^3\left(\frac{\alpha}{2}\right)-\cos\left(\frac{\alpha}{2}\right)\sin^2\left(\frac{\alpha}{2}\right)\right)+\frac{1}{\mu}\left(\sin^3\left(\frac{\alpha}{2}\right)-\frac{7}{2}\sin\left(\frac{\alpha}{2}\right)\cos^3\left(\frac{\alpha}{2}\right)\right)\right]<0 \tag{6}$$

Therefore, after obtaining the values of $J$-integral, $K_{\mathrm{I}}$ and $K_{\mathrm{II}}$ are estimated followed by determination of crack propagation angle $a$ using Eq. (5).

### 2.2.2 Fatigue crack growth model

Paris law is the most basic crack growth law. It is given by equation (7) as follows. Here, $C$ and $n$ are material constants. But, it does not consider the effect of crack closure phenomenon.

$$\frac{da}{dN}=C\Delta K^n \tag{7}$$

A number of other crack growth laws have been developed relating the rate of crack growth to the stress intensity factors. The well-known generalized NASGRO 2.0 equation is a modified Forman Law and is defined as [8]:

$$\frac{da}{dN}=\frac{C(1-f)^n\Delta K^n\left(1-\frac{\Delta K_{th}}{\Delta K}\right)^p}{(1-R)^n\left(1-\frac{\Delta K}{(1-R)K_C}\right)^q} \tag{8}$$

where $C$, $n$, $p$ and $q$ are empirical material constants, $R$ is stress ratio of the fatigue loading, $K_{\mathrm{C}}$ is critical stress intensity factor in plane stress condition, $\Delta K_{\mathrm{th}}$ is

threshold stress intensity factor, $\Delta K = K_{max} - K_{min}$ is the stress intensity factor range in fatigue loading, $N$ is number of cycles, d$a$ is crack extension length and $f$ is crack closure effect parameter. The above equation may be reduced to the Paris equation by setting the parameters $p$ and $q$ to zero without considering the effect of crack closure i.e. $f = R$ for $0 < R < 1$.

The fracture parameters of the aluminium alloy 2024-T3 are given in Table 1 and it is taken from Ref [8]

**Table 2.1:** Fracture Parameters of Aluminium alloy 2024-T3 [8]

| $\sigma_u$ (MPa) | $\sigma_y$ (MPa) | $K_{IC}$ (MPa mm$^{0.5}$) | $K_C$ (MPa mm$^{0.5}$) | C | $n$ | $p$ | $q$ | $f$ | $\Delta K_{th}$ (MPa mm$^{0.5}$) |
|---|---|---|---|---|---|---|---|---|---|
| 452 | 334 | 1015 | 1050 | 3.6e-11 | 3.282 | 0.5 | 1 | 0.39584 | 101.5 |

For mixed mode problems, the effective stress intensity factor range, $\Delta K_{eff}$, can be used instead of $\Delta K$, which is evaluated as shown in Eq. (9) [8]:

$$\Delta K_{eff} = \sqrt{(K_I^2 + 2K_{II}^2)} \tag{9}$$

Having obtained the stress intensity factors along with other known material parameters, Eq. (8) can be used to calculate fatigue crack growth lives of the cracked panels in mixed mode conditions.

After integrating Paris law equation, we will get following Eq. (10) [13]. It will give crack propagation life. Here $N_p$ stands for propagation life. Parametes $a_0$ and $a_f$ are initial and final crack length. $C$ is material constant.

$$N_p = \frac{\ln\left(\frac{a_f}{a_0}\right)}{Cf^2\left(\frac{a_0}{W}\right)(\Delta\sigma)^2\pi} \tag{10}$$

### 2.2.3 Finite Element Modeling 2D specimens

#### 2.2.3.1 Straight Edge Crack Modeling

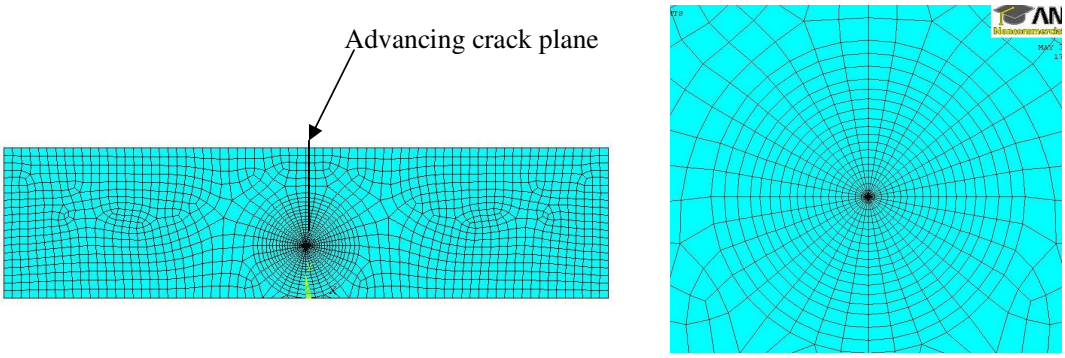


(a) (b)

**Fig. 2.4:** Finite Element Model of Straight Edge Cracked Specimen (a) Meshed finite element model (b) Zoomed portion of mesh near crack tip

For carrying out finite element analysis ANSYS 12.1 package is used. Figure 2.4 shows the finite element model of the edge crack specimen having a straight crack. The fully discretized model is shown in Fig. 2.4a. Very fine meshing is done around the crack tip as shown in Fig. 2.4b. The model consists of 1786 elements in total. Around the crack tip, 19 radial elements are used and 36 elements along circumferential divisions are employed to capture high stress gradients around the crack tip. Along radial direction, the element length is in geometric progression, with crack tip element length being equal to $0.001t$ and that of the last element is $0.18t$ (see Fig. 2.4b). Free meshing is done in the remaining part of the plate. The model is meshed with 8-node quadrilateral element (PLANE183) and the plate is subjected to an in plane load of 50 MPa. The problem is then analyzed with appropriate boundary conditions.

Every time the crack is incremented by 0.5 mm along the crack plane (see Fig. 2.4a) and the model is rebuilt with new crack tip location followed by SIF determination. The SIF is evaluated from $J$-integral which in turn is obtained from

finite element analysis. As SIF is obtained at different crack advancements, using Forman's law the number of cycle is estimated both analytically and from FEM.

#### 2.2.3.2 Inclined Edge Crack Modeling

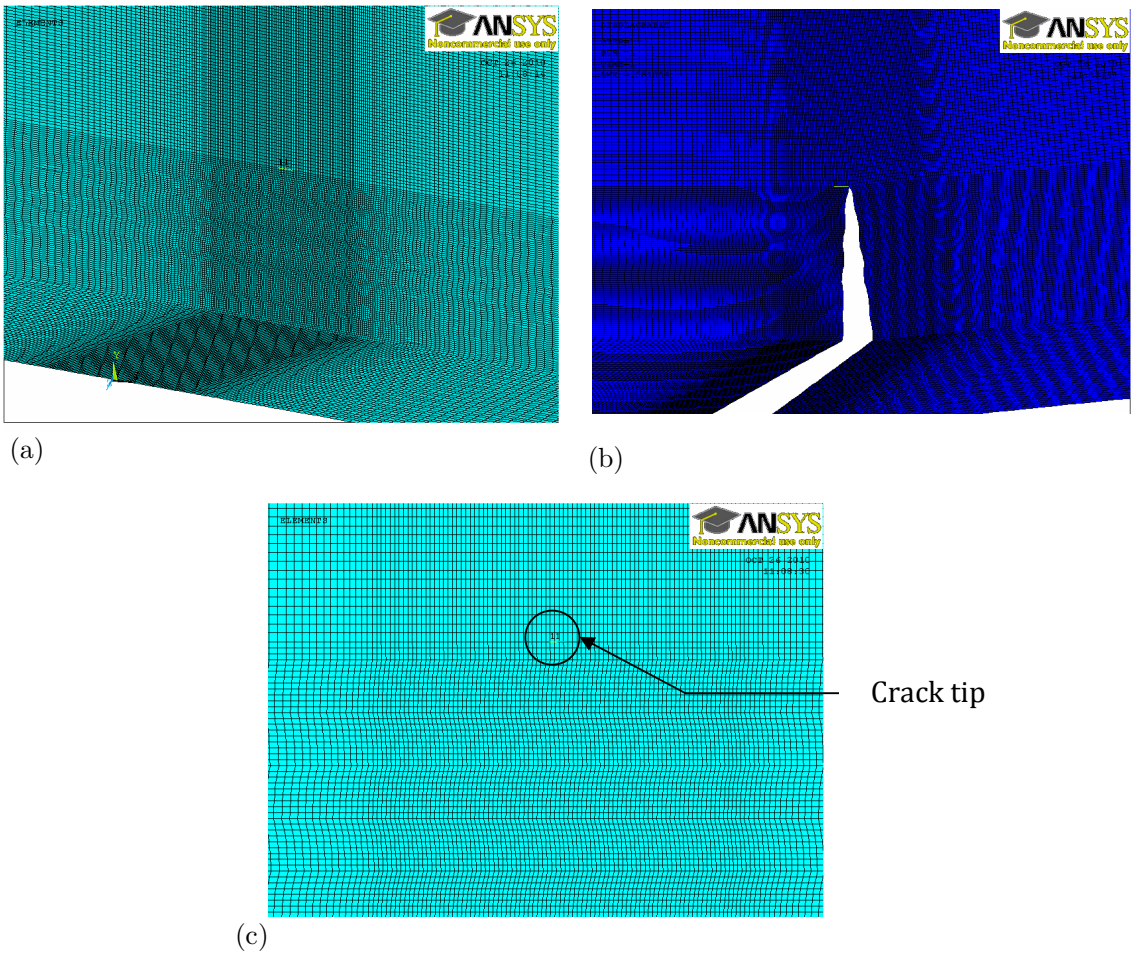


(a) (b)

(c)

**Fig. 2.5:** Finite Element Model of Inclined Edge Cracked Specimen (a) Meshed finite element model (b) Crack tip deformation after crack growth (c) Fine mesh around crack tip

Every time the crack is incremented The Fig. 2.5 shows the finite element model of the inclined edge crack specimen. Figure 2.5a shows the complete meshed model. The Fig. 2.5b shows the deformed model after the crack growth. Figure 2.5c shows the fine mesh created around the crack tip similar to that adopted in Ref. [11]. The 2-D model is meshed with 8-noded quadrilateral element (PLANE183) and the plate

is subjected to an in plane load of 50 MPa with appropriate boundary conditions. Every time crack front is incremented by 0.5 mm along the direction determined using MTS criterion. Then the model is rebuilt around new crack front location. To create the fine meshing around the crack tip, a band of area total 10 mm in length, 5mm on both sides of the crack face, is created along the crack. Very fine meshing is employed in this band. A spacing ratio of 0.05 is used for the mesh surrounding the band of fine mesh. Structured meshing pattern is employed for inclined edge crack unlike the circular pattern for the straight edge crack model. This is because it is very difficult to create mapped meshing for inclined edge crack model using circular meshing pattern for an each crack increment. After the meshing along with an appropriate boundary condition analysis is executed. Firstly $J$-integral value is directly obtained from Ansys. From the obtained $J$-integral value and displacements of the coincident nodes just before crack tip, the crack propagation angle $a$ and SIF is calculated. Then using Forman's law, the numbers of cycles are estimated.

## 2.3 Three-Dimensional Analysis

### 2.3.1 Introduction

In the real life, during actual crack propagation, the real crack front shape along the thickness is curved one. In two-dimensional analysis, we are not considering the thickness of panel. In order to get more realistic and accurate results, we should consider three-dimensional modeling. In this section, three dimensional analysis of unrepaired panel having straight and inclined center crack has been considered. The numbers of cycles are estimated. Finite element method is employed for getting the solution. Analysis has been carried out using Ansys 12.1 and Zencrack 7.6 finite element program. Meshing around the crack tip is very important and critical aspect during the analysis. Since, there is singularity at the crack tip, i.e. stresses reach infinity, meshing around the crack tip has to be fine and gradually increasing. Before going to further part of analysis, let us have some information regarding Zencrack 7.6 and details about the procedure followed for analysis.

### 2.3.2 Introduction to Zencrack

Zencrack is a state-of-the-art software tool for 3D fracture mechanics simulation [16]. The program uses finite element analysis to allow calculation of fracture mechanics parameters such as energy release rate, stress intensity factors and *J*-integral. This is achieved by automatic generation of focused cracked meshes from uncracked finite element models. In addition, a crack growth methodology is included that provides non-planar crack growth prediction for fatigue and time-dependent load conditions via automated adaptive meshing techniques.

The pre-processing for analysis of a cracked structure is significantly faster with Zencrack compared to generating a cracked model in a graphical pre-processor. This is because Zencrack requires only an uncracked mesh rather than a detailed cracked model. Preparation for a Zencrack analysis requires completion of two steps [16]:

a. Generation of Uncracked Mesh
b. Creating Zencrack input file

The uncracked mesh should be a valid mesh for the intact component. The Zencrack input file contains the ancillary information to convert the uncracked mesh to a cracked mesh and carry out the analysis.

### 2.3.3 Crack Blocks

A crack-block approach is then used to introduce one or more crack fronts into the uncracked mesh [16]. The term crack-block refers to a collection of brick elements stored as a unit cube. The arrangement of these crack-blocks is such that in their unit cube form they contain either a quarter circular or through crack front on one face. Part of this face is allowed to open up under loading giving the opening crack face within the crack-block. The meshing procedure is one of replacement of one or more 8 or 20 noded brick elements in a user supplied uncracked mesh by crack-blocks. During the mapping process to introduce the crack-blocks the user can control the size and shape of the generated crack front section for each crack-block. The initial crack front derived from a quarter circular crack-block may be elliptic, for example. Crack-blocks can be connected together to form distinct crack fronts of the required size in the cracked mesh.

Typical crack-blocks are as shown in Fig. 2.6 below [16]:

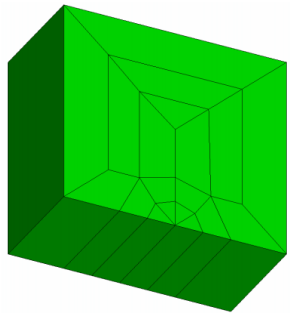

(a) Crack-block s02_t19x1

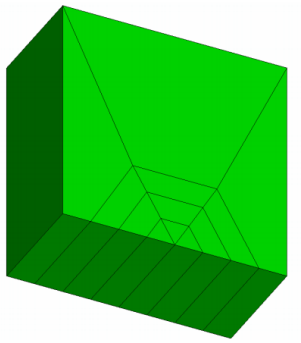

(b) Crack-block s05_t12x1

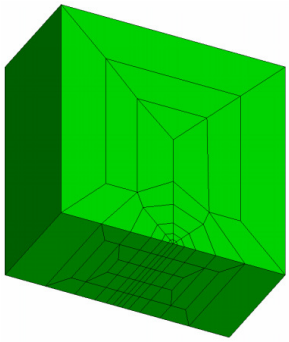

(c) Crack-block s_t111x5

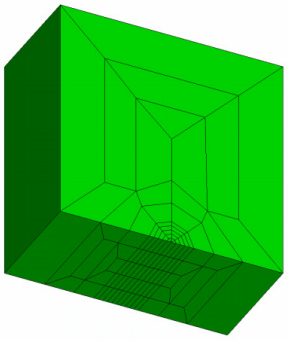

(d) Crack-block s_t151x5

**Fig. 2.6:** (a) Various types of crack-blocks [16]

### 2.3.4 Overall methodology of three-dimensional analysis

For three-dimensional analysis, an Ansys 12.1 and Zencrack 7.6 finite element code has been used. The following flowchart explains the basic procedure of analysis. The basic steps involved in the analysis are explained below through flowchart below:

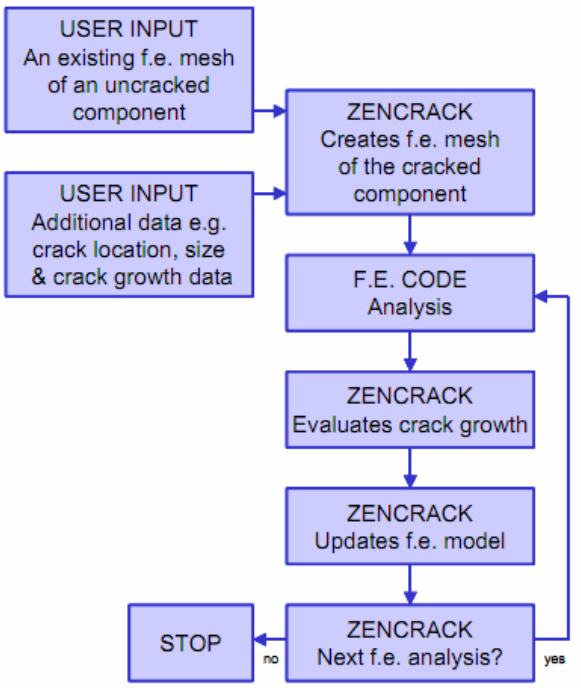


**Fig. 2.7:** Flowchart of overall methodology of three-dimensional analysis [16]

i. For analysis we need two files namely "Uncracked mesh file" having .ans as its extension and "Zencrack command file", commonly called as "zcr file", having .zcr as extension.

ii. Uncracked mesh file contains the APDL (Ansys Parametric Design Language) commands for creating the uncracked meshed model whereas Zcr file contains the commands required by Zencrack for the crack propagation analysis.

iii. In zcr file we have to specify the element numbers and corresponding node numbers which we have to replace with the crack block. "*CRACKFRONT" command is used for that. So, this creates the crackfront and hence cracked mesh. The details of each command will be discussed in later sections.

iv. Also, we have to include commands related with crack growth data, mesh relaxation, material properties, loads etc. in zcr command file.

v. After creating the uncracked mesh file and zcr file for particular model, both the files are saved in one folder.

vi. After that in Zencrack command window, analysis is started using the command "runzcr76 –j=zcrfilename int", where "zcrfilename" is the actual name of the zcr file.

vii. After completing the analysis, it generates one file having ".rep" as its extension. This is the main results file of Zencrack. It is a notepad file.

viii. We can get the results in more systematic format in excel sheet by using one of the available utility functions. Command for that is "runzcr76 process". This generates the excel sheet having results in it.

ix. We can get the required graphs by using the available "process growth" template. We have to just copy the necessary data in it to get the graphs of the "Sum of da Vs. Number of cycles".

### 2.3.5 Finite element modeling of three-dimensional models

In this section the finite element modeling of straight and inclined center crack specimen has been discussed. While modeling the initial uncracked panel, care has to be taken to make the mesh suitable according to the orientation of the crack. This is because crack blocks have to be orientated suitably to get the required initial crack.

#### 2.3.5.1 Unrepaired Panel with Straight Center Crack

The following Fig. 2.8 shows the dimensions and finite element meshed model of panel after inserting crack blocks. As shown in figure length of panel is 100mm and width is 50mm. Crack length (2a) is 10mm. The material used for panel is Aluminium-2024 T3. The modeling is carried out using Ansys 12.1.

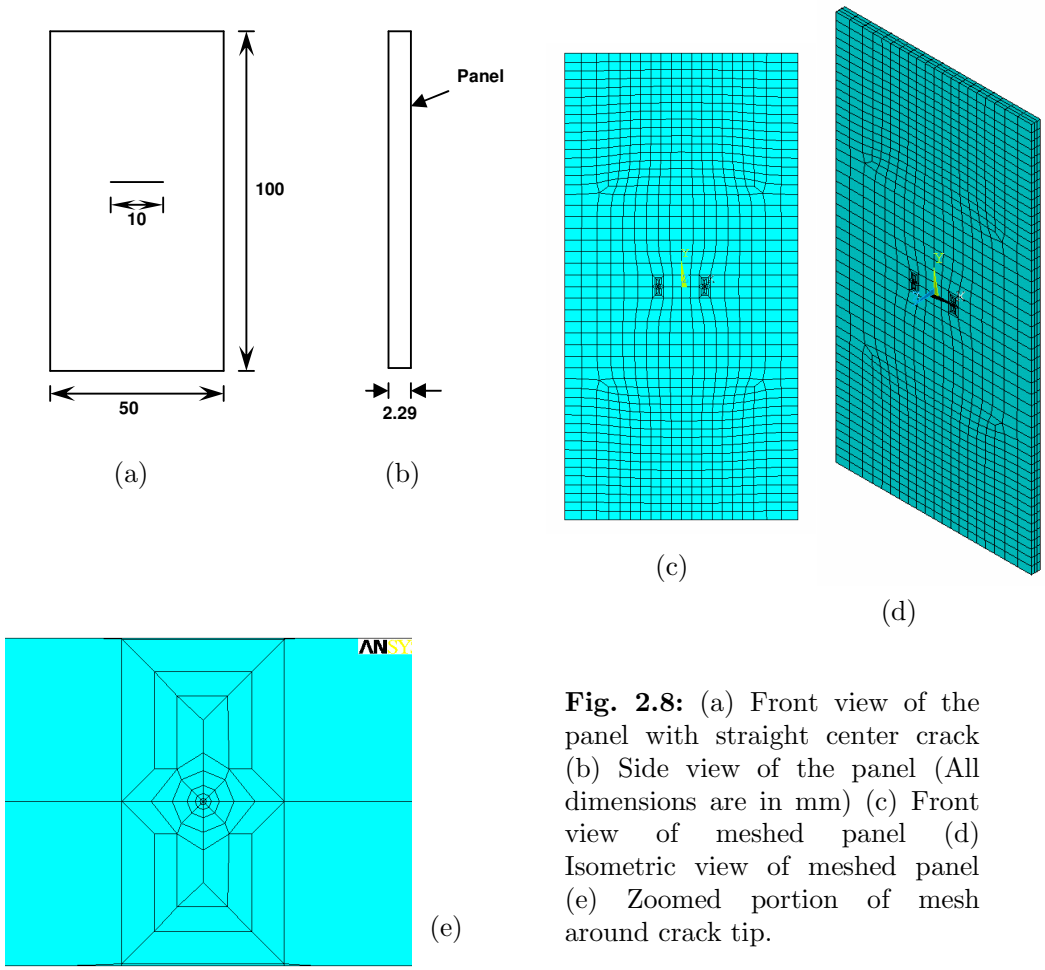


**Fig. 2.8:** (a) Front view of the panel with straight center crack (b) Side view of the panel (All dimensions are in mm) (c) Front view of meshed panel (d) Isometric view of meshed panel (e) Zoomed portion of mesh around crack tip.

Element type used is 8-node solid element, in Ansys terminology it is SOLID185. Three elements are used along the thickness of panel. The standard type of crack block is used. Crack block used is s02_t19x1. The lower end of the panel is fixed and is subjected to in-plane load of 118 MPa at the top end. The analysis has been carried by using both Paris as well as by Forman's law.

#### 2.3.5.2 Unrepaired Panel with Inclined Center Crack

Analysis has been carried out for the unrepaired panel having inclined crack for various crack inclination angles of 30°, 45° and 60°. The initial finite element mesh for an uncracked panel having different crack inclination angle is quite similar. Analysis has been carried out for unrepaired panel, single side patch and double sided patch models with crack inclination angles of 30°, 45° and 60°.

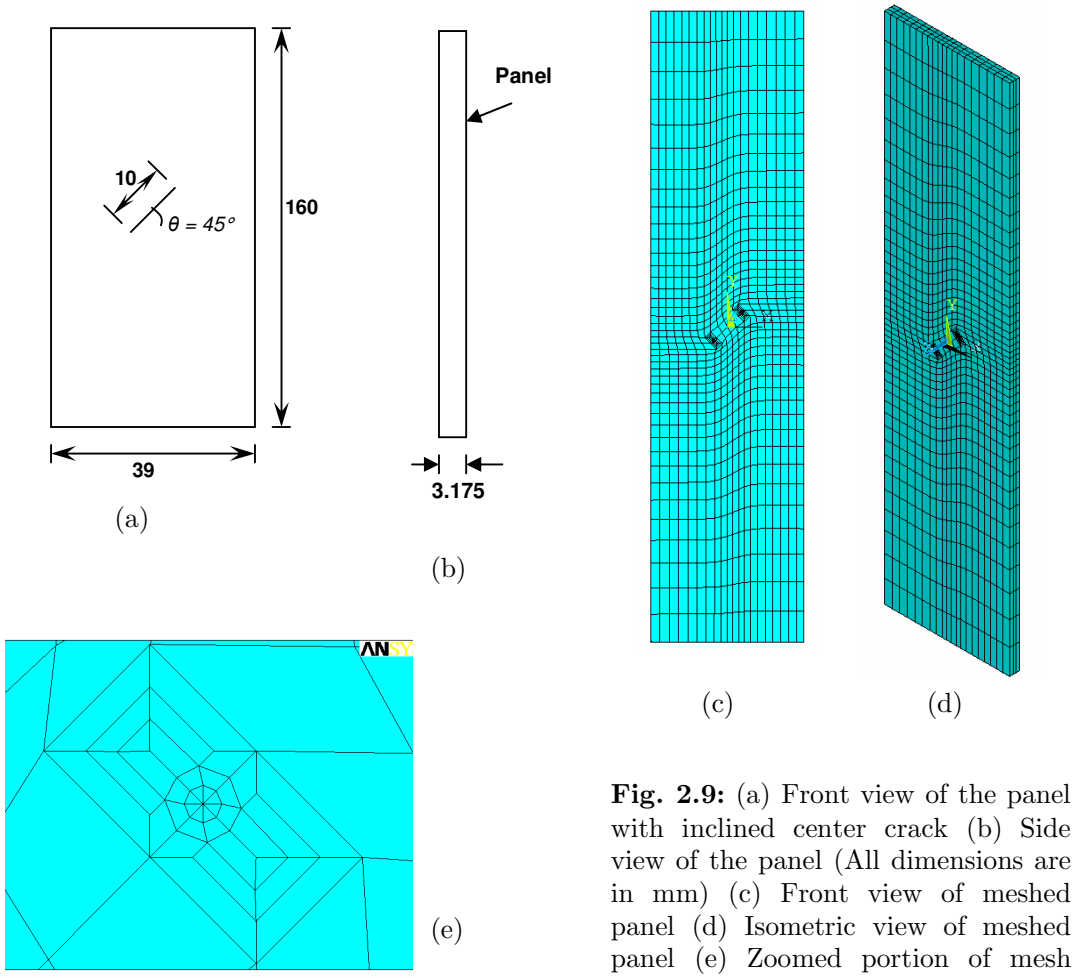


**Fig. 2.9:** (a) Front view of the panel with inclined center crack (b) Side view of the panel (All dimensions are in mm) (c) Front view of meshed panel (d) Isometric view of meshed panel (e) Zoomed portion of mesh around crack tip.

The above fig. 2.9 shows the dimensions and the finite element meshed model of inclined crack panel. The length of the panel is 160mm and the width is 39mm. Thickness of the panel is 3.175mm. Initial crack length (2a) is 10mm. The $\vartheta$ is the crack inclination angle. Here, initial uncracked mesh is made such that the crack blocks are orientated in a manner to get the inclined crack of required length and inclination. The analysis has been carried out for crack inclination angles ($\vartheta$) of 30°, 45° and 60°. The material used for panel is Aluminium-2024 T3.

### 2.3.6 Calculation of fracture parameters

In Zencrack, the energy release rate magnitude and its corresponding direction as the criterion for calculating crack growth. The energy release rate along 3D crack front is calculated using two methods: a) The evaluation of change in strain energy for various virtual crack extensions (VCEs) at the crack front(s). (b) The use of nodal displacements close to the crack front to calculate stress intensity factors for the opening, sliding and tearing mode, followed by conversion to the equivalent energy release rate.

### 2.3.7 Virtual crack extension method

The calculation of energy release rate at a crack front via finite element analysis was first demonstrated by Parks and Helen [16, 18] in independent publications. The method which they both presented commonly referred to as the stiffness derivative or virtual crack extension technique, was formulated specifically for finite element applications. The change in energy is calculated for a virtual crack extension at the crack front. The accuracy of this method is known to depend upon the magnitude of the applied virtual crack extensions.

The calculation of the energy release rates using virtual crack extensions is implemented in many finite element codes and is often generalized to calculate J-integrals. Zencrack takes advantage of the available implementation in the interfaced finite element codes rather than providing a stand-alone VCE capability driven by the basic results of the finite element analysis.

At any node on a 3D crack front a “normal plane” can be defined. This is a plane that is orthogonal to the crack front tangent at the node. A series of virtual crack extensions in the normal plane will produce a distribution of energy release rates. At some angle to the local crack plane the energy release rate will be a maximum. Gmax denotes the maximum energy release rate. The value of Gmax and the corresponding angle must be calculated for use in crack growth prediction.

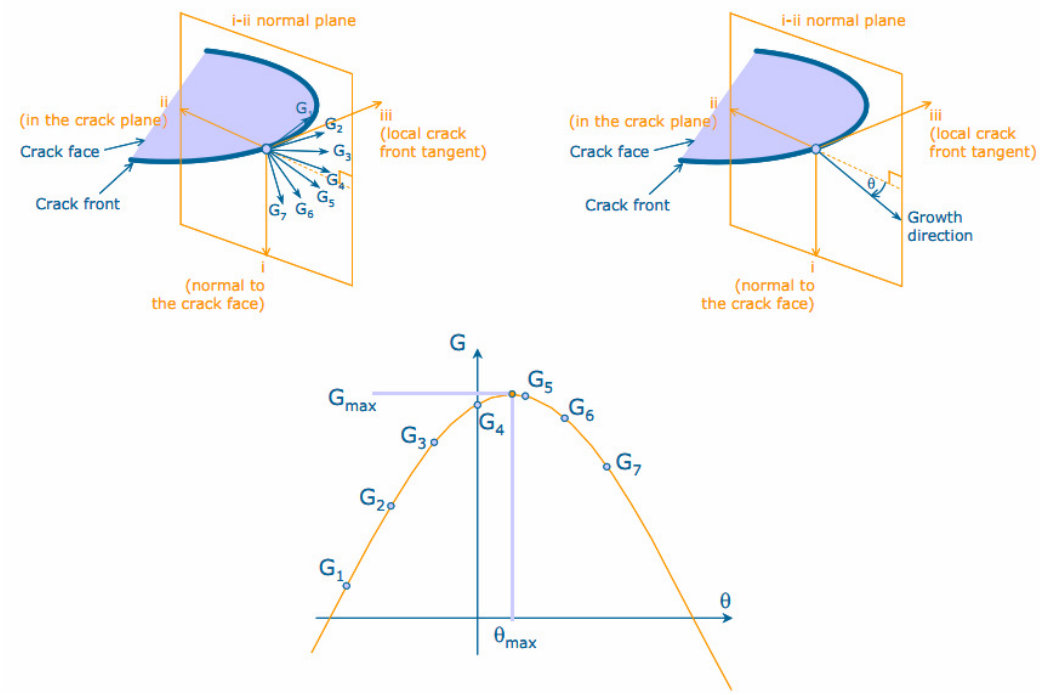


**Fig. 2.10:** Virtual crack extension method [16]

### 2.3.8 Prediction of fatigue life

The Paris law is used to calculate the number of cycles. The crack growth integration takes each corner node on the crack front in turn and calculates the growth magnitude and direction for the node. This allows the crack to be advanced through the model. The integration is generally a two-pass process to ensure that all nodes grow by the same number of cycles from one finite element analysis to the next. In general the da will vary from node to node along the crack front [16]. During the update of the crack front to a new position, the midside nodes are positioned in such a way as to try to obtain a smooth crack front. The crack front

nodes may be shifted along the crack front in order to maintain correct surface positions and spacing along the crack front.

## 2.4 Results and Discussion

### 2.4.1 Results of Two-Dimensional analysis

In this section, the results for the two dimensional analysis have been discussed. Results are obtained for edge crack specimens with crack inclination angles of 30°, 45° and 60°.

#### 2.4.1.1 Straight edge crack model analysis

The SIF is calculated both analytically as well as by FEM for different crack growth lengths. The variation of SIF with respect to crack growth length is shown in Fig. 2.11 (a). The SIF evaluated analytically and from FEM are matching very closely for different crack growth lengths. The variation of the crack growth length versus number of cycles is shown in Fig. 2.11 (b). There is a close match between analytical and FEM results. Slight variation is observed nearer to the critical crack region.

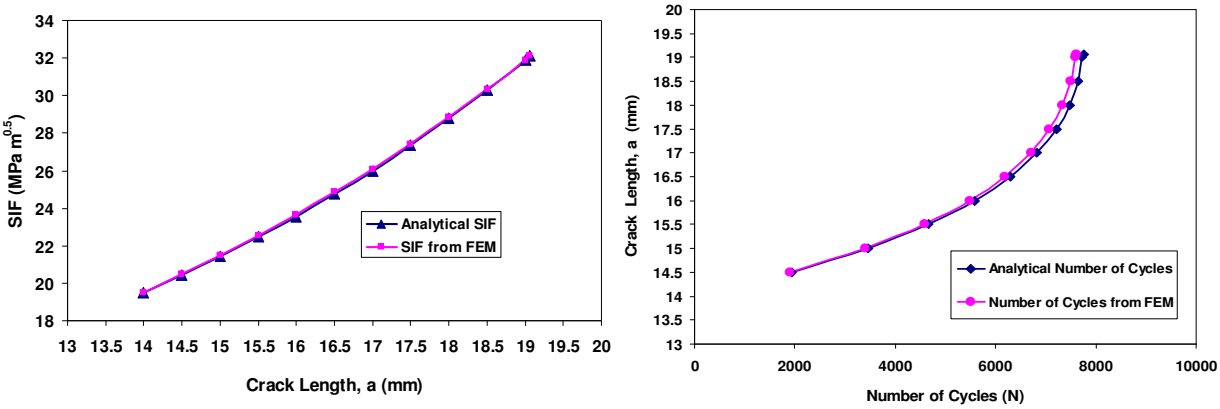


(a) (b)

**Fig. 2.11:** (a) Variation of the SIF with crack length for straight edge crack model and (b) Variation of the Crack length with number of cycles for straight edge crack model

#### 2.4.1.2 Inclined edge crack model analysis

##### 2.4.1.2.1 60° crack inclination angle

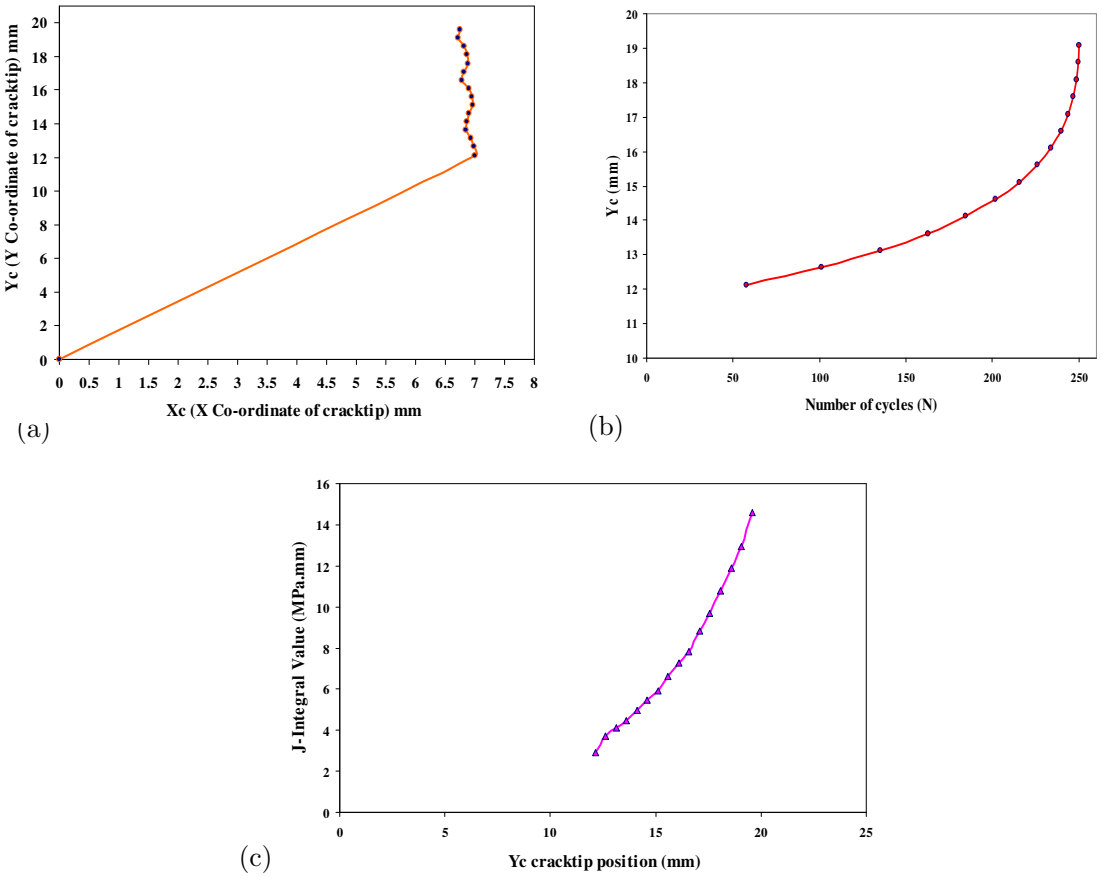


**Fig. 2.12:** (a)Crack propagation path for the 60° inclined edge crack model (b)Variation of the Yc crack tip position with number of cycles for the 60° inclined edge crack model and (c) Variation of *J*-intergral value with Yc crack tip position for the 60° inclined edge crack model

Figure 2.12 (a) shows the crack propagation path for the 60° inclined edge crack model. It gives the information about the predicted crack propagation path. It is the graph of Yc, (Y co-ordinate of the crack tip), versus Xc (X co-ordinate of the crack tip). Figure 2.11 (b) gives the variation of the number of cycles with respect to the Yc. Figure 2.11 (c) gives variation of the *J*-integral value with the Yc. It can be observed from the Fig. 2.11 (b) that number of cycles is very less. It takes very

less time to fail. The total number of cycles before failure is 250 for the given geometry and loading.

#### 2.4.1.2.2 45° crack inclination angle

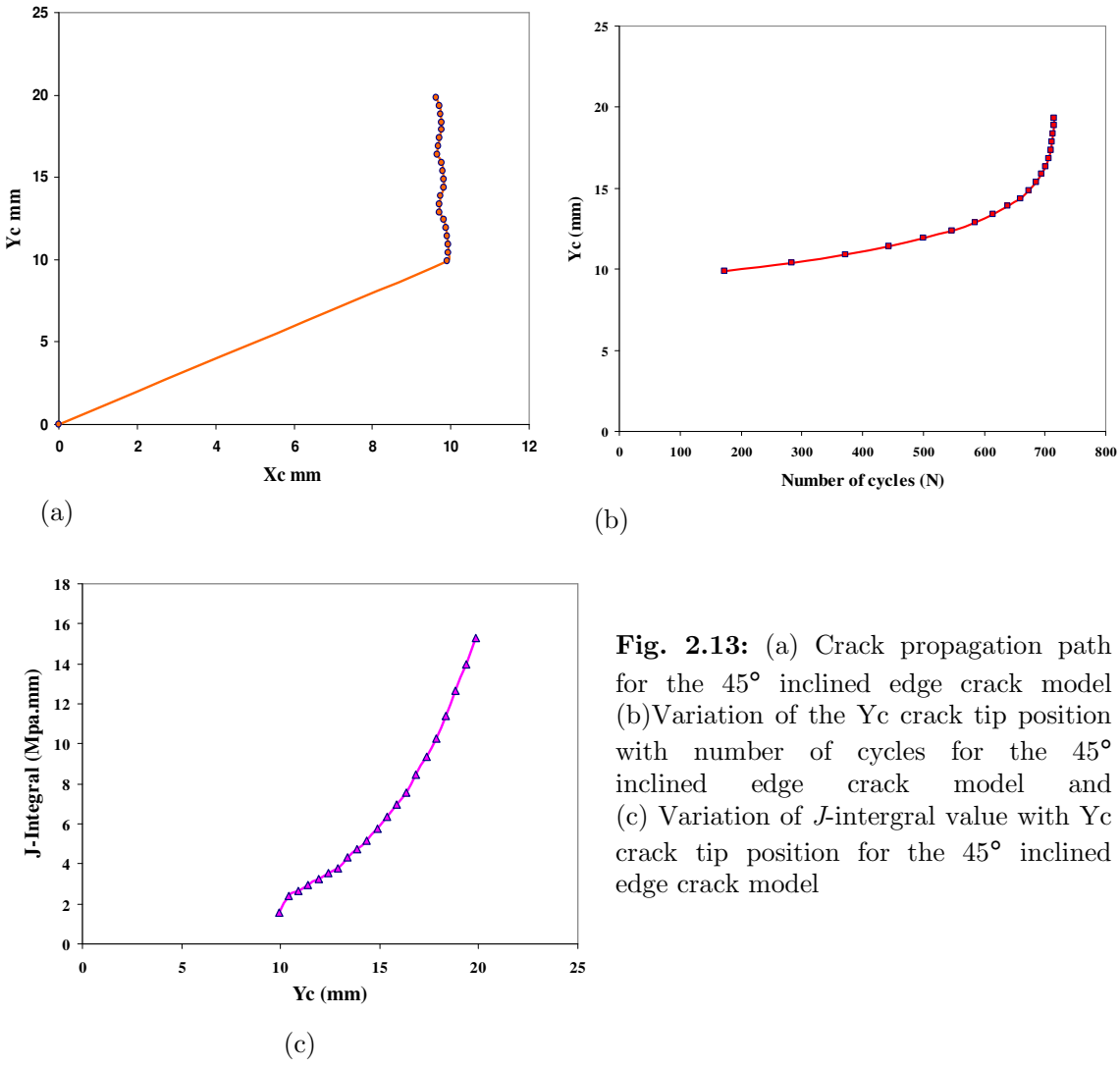


**Fig. 2.13:** (a) Crack propagation path for the 45° inclined edge crack model (b)Variation of the Yc crack tip position with number of cycles for the 45° inclined edge crack model and (c) Variation of *J*-intergral value with Yc crack tip position for the 45° inclined edge crack model

Figure 2.13 (a) shows the crack propagation path for the 45° inclined edge crack model. It gives the information about the predicted crack propagation path. It is the graph of Yc, (Y co-ordinate of the crack tip), versus Xc (X co-ordinate of the crack tip). Figure 2.13 (b) gives the variation of the number of cycles with respect to the Yc. Figure 2.13 (c) gives variation of the J-integral value with the Yc. It can

be observed from the Fig. 2.13 (b) that number of cycles is more than that for the 60° crack inclination angle. The total number of cycles before failure is 715 for the given geometry and loading conditions.

#### 2.4.1.2.3 30° crack inclination angle

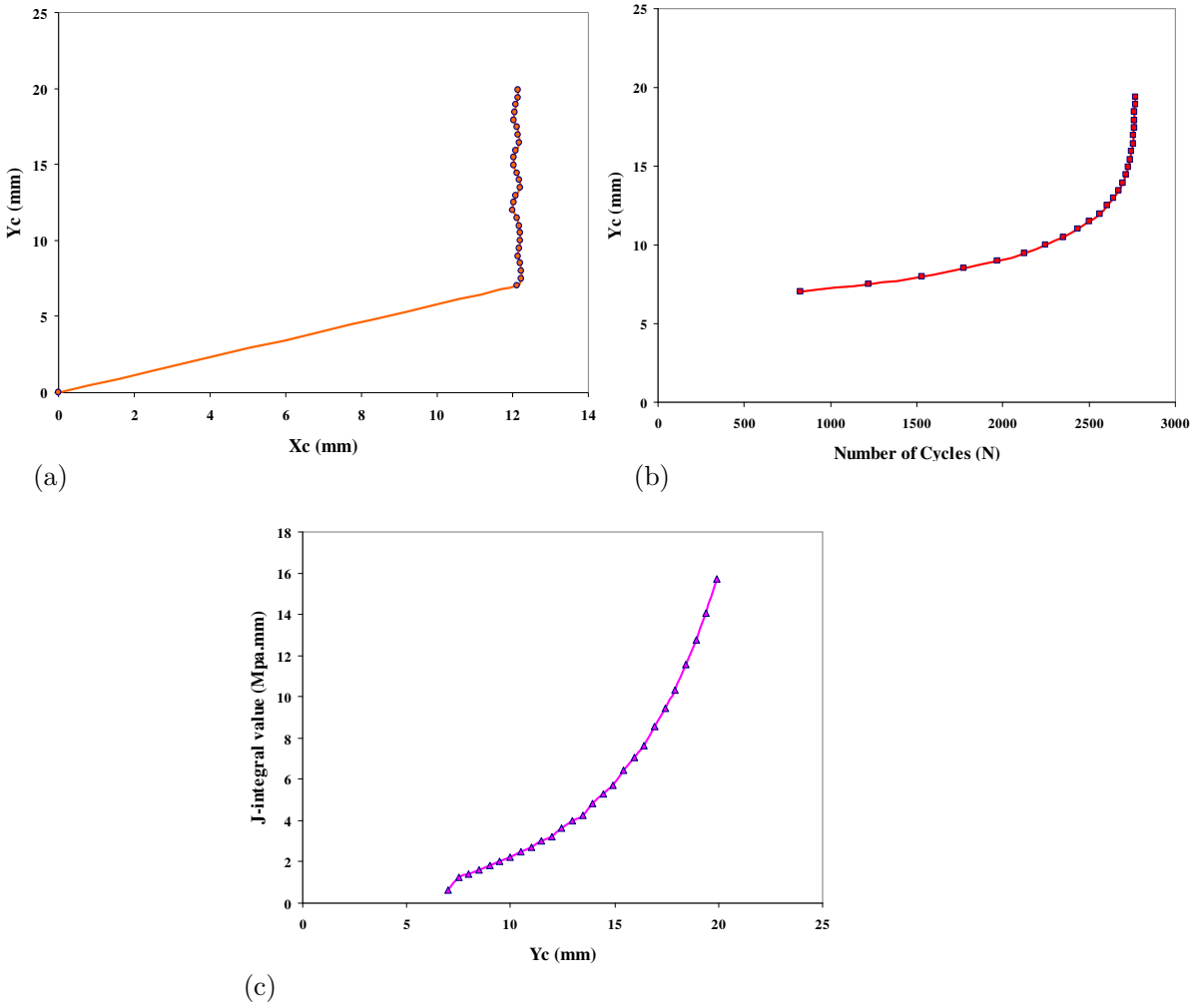


**Fig. 2.14:** (a) Crack propagation path for the 30° inclined edge crack model (b)Variation of the Yc crack tip position with number of cycles for the 30° inclined edge crack model and (c) Variation of *J*-intergral value with Yc crack tip position for the 30° inclined edge crack model

Figure 2.14 (a) shows the crack propagation path for the 30° inclined edge crack model. It gives the information about the predicted crack propagation path. It is the graph of Yc, (Y co-ordinate of the crack tip), versus Xc (X co-ordinate of the crack tip). Figure 2.14 (b) gives the variation of the number of cycles with respect to the Yc. Figure 2.14 (c) gives variation of the *J*-integral value with the Yc. It can be observed from the Fig. 2.14 (b) that the number of cycles is comparatively much higher than that for 60° and 45° crack inclination angles. The total number of cycles is 2767 for the given geometry and loading conditions. Also, one can see that the rate of crack growth is slow in the initial stage. But, in later stage crack grows with very faster rate.

### 2.4.2 Results of Three-Dimensional analysis

The three dimensional analysis has been carried out for straight center crack and for inclined center crack models with crack inclination angles of 30°, 45° and 60°. The analysis has been carried out for unrepaired panel by using both, Paris law and Forman's law.

#### 2.4.2.1 Validation of Results

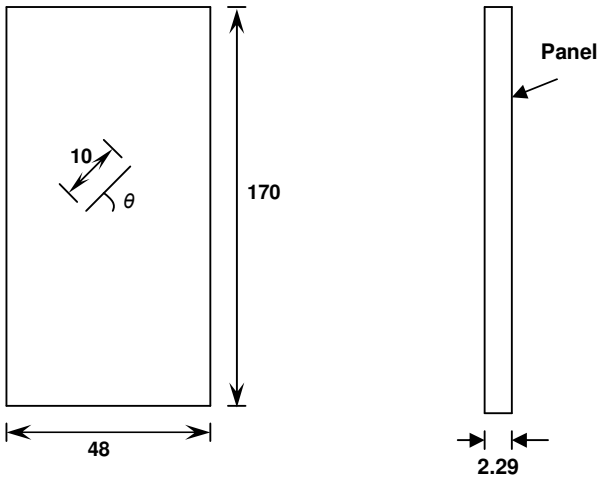


**Fig. 2.15:** (a) Front view of the inclined center crack panel (b) Side view of the panel (All dimensions are in mm)

In order to validate the results, analysis has been carried out for specimens shown in fig. 2.15. The obtained results are compared with the available results from reference [17]. Very small deviation has been observed and good match exists between them. By using Paris law, analysis is carried out for the specimen shown in fig. 2.15. It can be seen from fig. 2.16 (a) that number of cycles are 15846. The numbers of cycles from reference [17] are 16348. In order to check the crack growth data using Forman law, the d$a$/dN values obtained from zencrack and by formula are compared. The value of da/dN obtained from zencrack for one step in the analysis is 3.707E-5 while that obtained from the direct Forman law after substituting values is 3.68E-5. Hence, very good match exists between them.

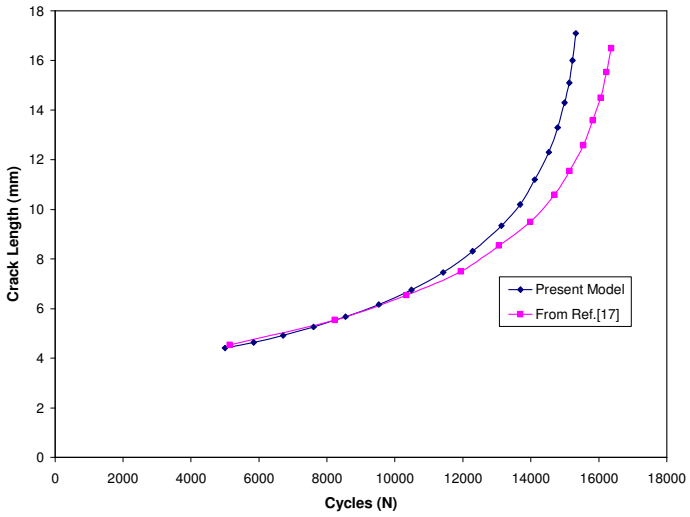


**Fig. 2.16:** Variation of sum of da with number of cycles for unrepaired panel for model from ref.[17]

Stress intensity factor values were validated for the panel model having straight center crack as shown in fig. 2.8 against the analytical equation. The analytical equation for SIF is given by eq. (11) below [13].

$$K_I = \sigma\sqrt{(\pi a)}\, f(\alpha) \tag{11}$$

where, $\alpha = \dfrac{a}{W}$ (12)

$$f(\alpha) = 1 + 0.128\alpha - 0.288\alpha^2 + 1.523\alpha^3 \tag{13}$$

The stress intensity factor $K_{\mathrm{I}}$ obtained from FEM is 480 MPa(mm)$^{0.5}$. The value of SIF obtained from the analytical eq. (11) is 481 MPa(mm)$^{0.5}$ for same geometry and loading conditions. Hence, there exists a very good match between the SIF values obtained from FEM and from analytical expression.

#### 2.4.2.2 Unrepaired panel model having straight center crack

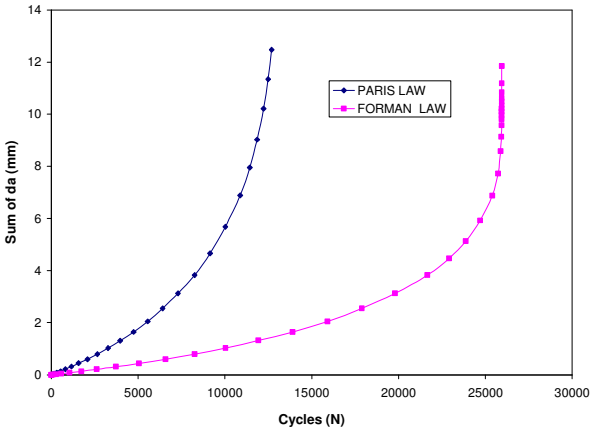


**Fig. 2.17:** Variation of sum of da with number of cycles for unrepaired panel having straight center crack

Fig. 2.17 shows the variation of sum of da (crack increment) with number of cycles for unrepaired panel. The results are obtained for both Paris law as well as Forman law. As can be seen from the figure, the numbers of cycles for Forman law are more. The number of cycles by using Paris law and Forman are 12698 and 25950 respectively.

#### 2.4.2.3 Results for Unrepaired panel model with inclined center crack

##### 2.4.2.3.1 Panel with 30° Crack Inclination Angle

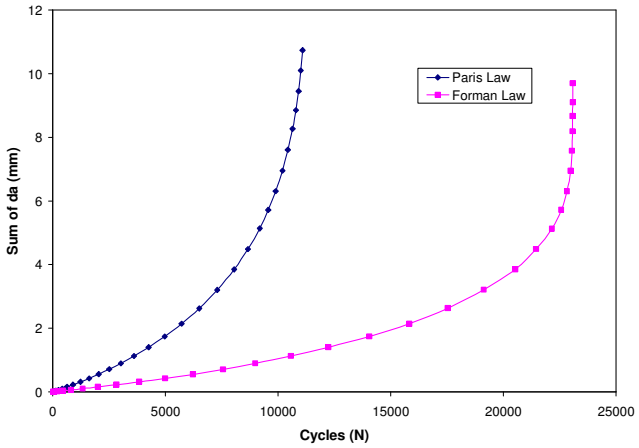


**Fig. 2.18:** Variation of sum of da with number of cycles for unrepaired panel having inclined center crack with crack inclination angle of 30°

Fig. 2.18 shows the variation of sum of da with number of cycles for unrepaired panel with inclined crack at 30°. The results are obtained for both Paris law as well as Forman law. As can be seen from the figure, the numbers of cycles for Forman law are more than Paris law. The number of cycles by using Paris law and Forman are 11087 and 23077 respectively.

##### 2.4.2.3.2 Panel with 45° Crack Inclination Angle

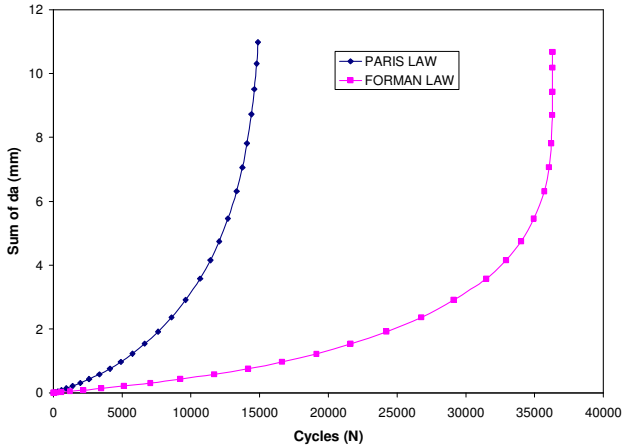


**Fig. 2.19:** Variation of sum of da with number of cycles for unrepaired panel having inclined center crack with crack inclination angle of 45°

Fig. 2.19 shows the variation of sum of da with number of cycles for unrepaired panel with inclined crack at 45°. The results are obtained for both Paris law as well as Forman law. As can be seen from the figure, the numbers of cycles for Forman law are more than Paris law. The number of cycles by using Paris law and Forman law are 14889 and 36309 respectively. As can be seen, numbers of cycles are more than that for 30° crack inclination angle.

#### 2.4.2.3.3 Panel with 60° Crack Inclination Angle

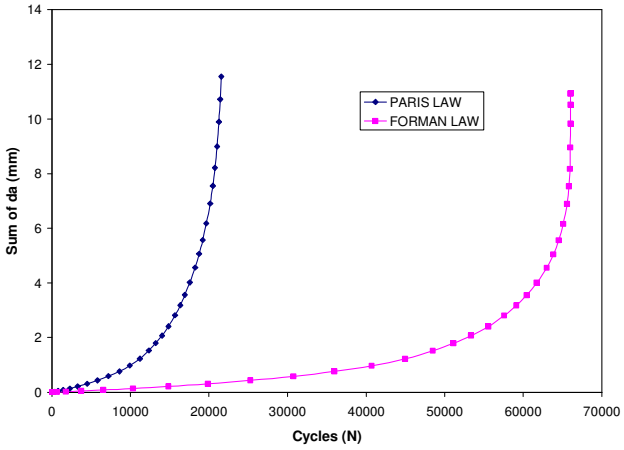


**Fig. 2.20:** Variation of sum of da with number of cycles for unrepaired panel having inclined center crack with crack inclination angle of 60°

Fig. 2.20 shows the variation of sum of da with number of cycles for unrepaired panel with inclined crack at 60°. The results are obtained for both Paris law as well as Forman law. As can be seen from the figure, the numbers of cycles for Forman law are more than Paris law. The number of cycles by using Paris law and Forman are 21584 and 66030 respectively. As can be seen, number of cycles are more than that for 30° and 45° crack inclination.

#### 2.4.2.4 Results for three dimensional analysis of edge crack model

In this section, results for three dimensional analyses of edge crack models shown in fig. 2.21 and 2.23 have been discussed.

##### 2.4.2.4.1 Straight edge crack results

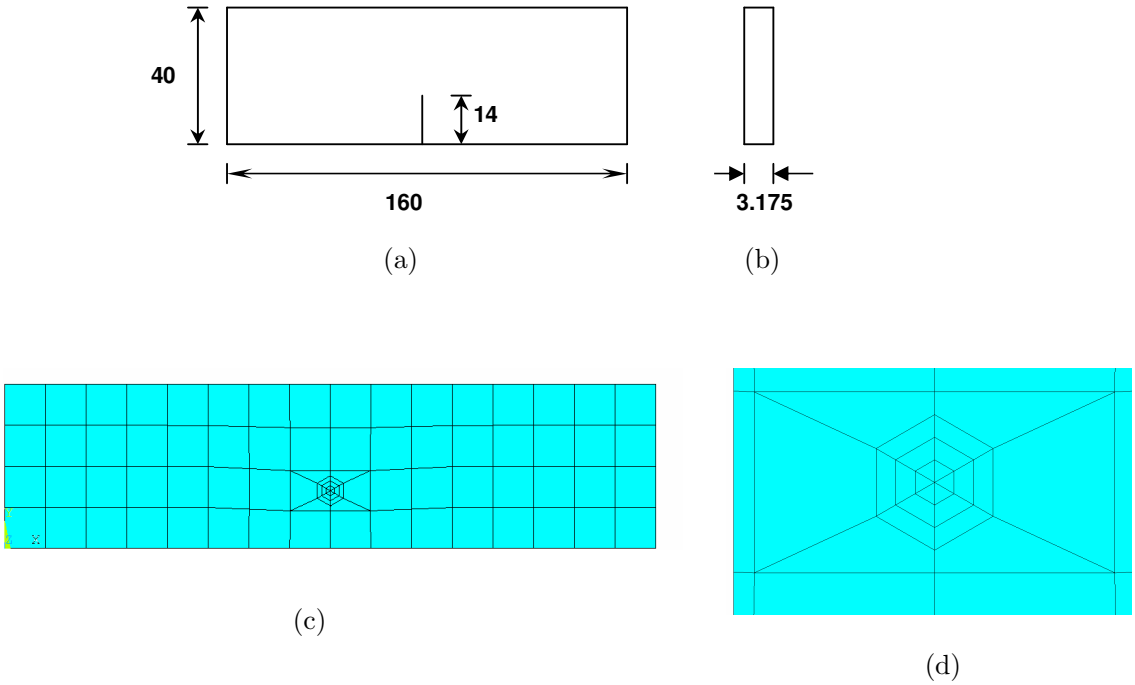


**Fig. 2.21:** (a) Front view of the panel with straight edge crack (b) Side view of the panel (All dimensions are in mm) (c) Front view of meshed panel (d) Zoomed portion of mesh around crack tip

Fig. 2.21 shows the dimensions and the finite element model of straight edge crack specimen. The length of the panel is 160mm and the width is 40mm. Thickness of the panel is 3.175mm. Initial crack length is 14mm. The standard type of crack-block has been used. Crack-block used is s05_t12x1.

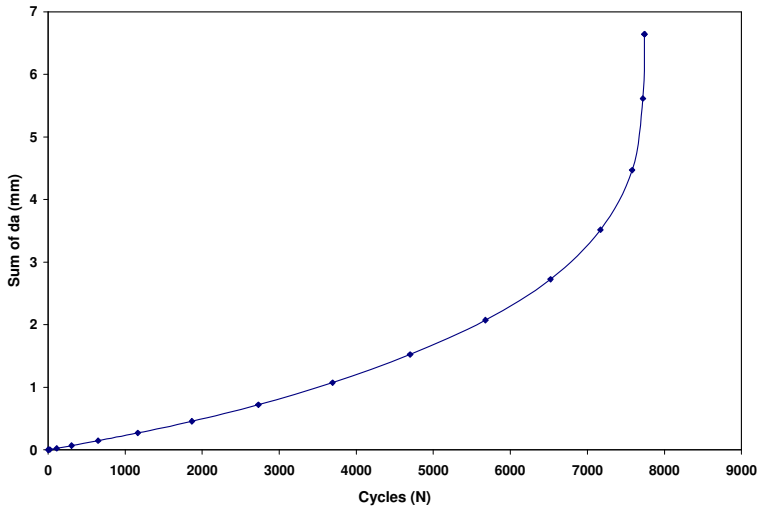


**Fig. 2.22:** Variation of sum of da with number of cycles for unrepaired panel having straight edge crack

Fig. 2.22 shows the variation of sum of da with number of cycles for straight edge crack model. From fig. 2.11 (b) and 2.22, we can see that there exists good match between the results of two-dimensional and three-dimensional analysis.

#### 2.4.2.4.2 Inclined edge crack results

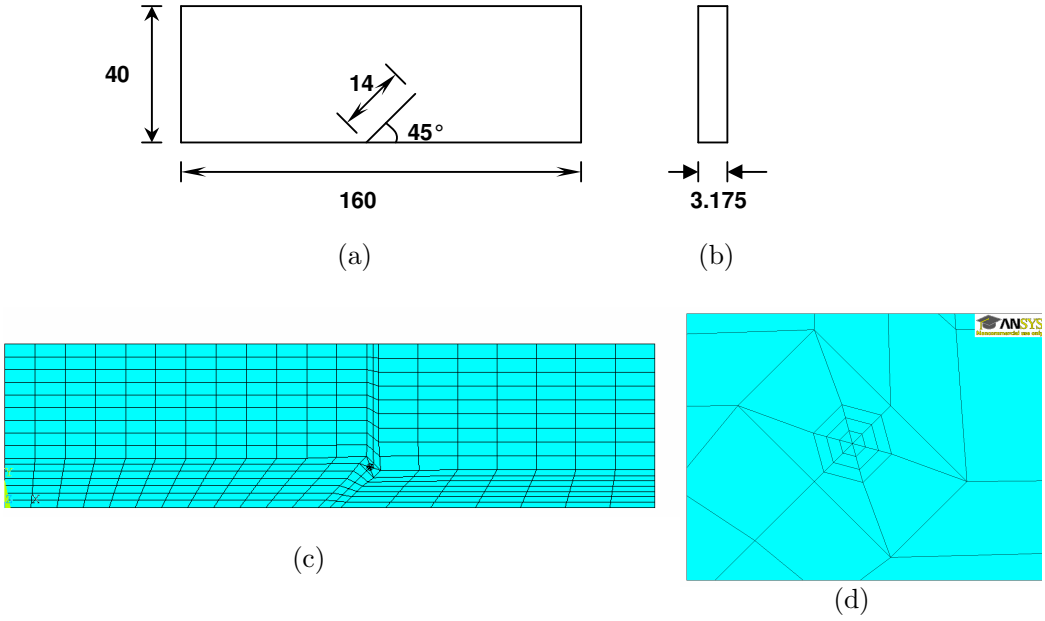


**Fig. 2.23:** (a) Front view of the panel with inclined edge crack (b) Side view of the panel (All dimensions are in mm) (c) Front view of meshed panel (d) Zoomed portion of mesh around crack tip

Fig. 2.23 shows the dimensions and the finite element model of inclined edge crack specimen. The length of the panel is 160mm and the width is 40mm. Thickness of the panel is 3.175mm. Initial crack length is 14mm. Crack inclination angle is 45°. The standard type of crack-block has been used. Crack-block used is s05_t12x1.

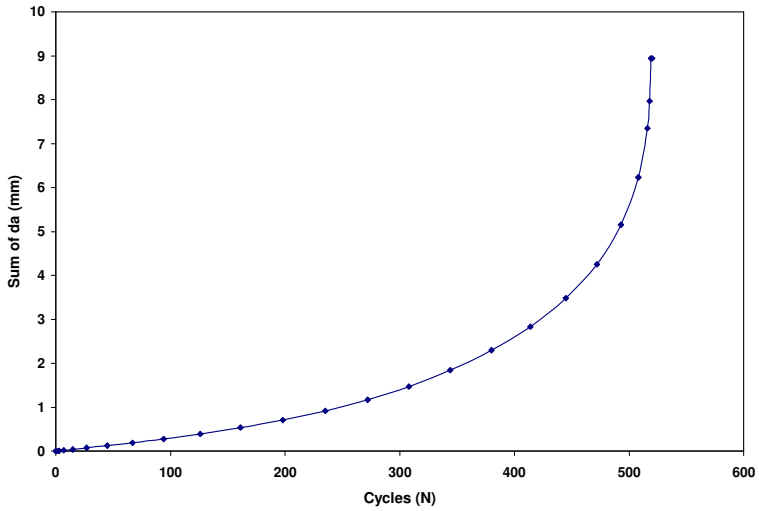


**Fig. 2.24:** Variation of sum of da with number of cycles for unrepaired panel having inclined edge crack with crack inclination angle of 45°

Fig. 2.24 shows the variation of sum of da with number of cycles for inclined edge crack model with crack inclination angle of 45°. From fig. 2.13 and 2.24, it can be seen that there is little deviation between the results of two-dimensional and three-dimensional results.

## 2.5 Closure

In this study, fatigue crack propagation analysis has been carried out for two dimensional as well as three dimensional models using finite element method. In two dimensional analyses, fatigue crack propagation in straight crack edge specimen and also inclined crack edge specimen is studied using finite element method. The crack propagation study has been carried out for the inclined edge crack specimens of 30°, 45° and 60° crack inclination angles. It is observed that there is not much significant difference in crack propagation trajectory for the inclined edge crack specimens having different crack inclination angles. The variation of the number of cycles with the $Y_C$ was studied. It is observed that the number of cycles increases with reduction of the crack inclination angle. The 30° crack inclination, model has got more number of cycles before failure than for 45° and 60° crack inclination models. The variation of the J-integral value with respect to the different crack growth positions has also been studied in this paper. It is observed that initially the *J*-integral value increases slowly but at later stage it increases at a faster rate.

Three dimensional analysis was carried out for the unrepaired panels having straight and inclined center crack. Three dimensional analysis is carried out by considering curved crack front shape. All the analyses have been carried out using both Paris law and Forman law. It can be seen that the number of cycles for inclined crack increases as initial crack inclination angle increases. The numbers of cycles are more for the 60° than that for 45° and 30°.

# Chapter 3

# Fatigue Crack Propagation Modeling of Patched Panel

## 3.1 Composite Patch Repair

Composite patch repair is mainly concerned with repairing of the damaged aircrafts or aircrafts having cracks on there bodies. The crack can appear because of many reasons. Body of the aircraft is mainly made up of Aluminum alloy-2024 T3. All metallic structures are prone to degradation by cracking and corrosion in service, particularly when design, manufacture or environmental protection is inadequate to meet actual serviced usage. In military aircraft fatigue cracking may be more of a problem than originally envisaged because of exposure to more severe usage (higher loading) than originally anticipated. Corrosion is a problem with older aircraft because of the use of susceptible alloys and inadequate corrosion-protective processes. Because of limited budgets and escalating replacement costs, many military aircraft are being maintained in service well past their planned life.

When today's aircraft reach the end of their service life, fatigue cracks are found to have developed along rivet holes and other highly stressed regions of the aircraft. In order to extend the life of these aircraft, repairs have been made to arrest these cracks. Composite doublers or repair patches provide an innovative repair technique, which can enhance the way aircraft are maintained. Instead of riveting multiple steel or aluminum plates to facilitate an aircraft repair, a single composite doubler is bonded to the damaged structure. Adhesively bonded composite repairs have many advantages over mechanically fastened repairs (Baker and Jones, 1988)

[14]: (i) no new stress concentration created by new rivet holes; (ii) high stiffness-to-weight and strength-to-weight ratios of the patch, thus reducing drag; (iii) patches are readily formed into complex shapes, permitting the repair of irregular components; (iv) high fatigue and corrosion resistance of the composite; and (v) potential time savings in installation. This repair technique has been primarily used in the area of military aviation for extending the service life of aircrafts.

### 3.2 Objective of Bonded Repairs

Bonded repair of metallic aircraft structure is used to extend the life of flawed or under-designed components at reasonable cost. Such repairs generally have one of three objectives: fatigue enhancement, crack patching or corrosion repair.

### 3.3 Types of Bonded Repairs

There are two types of repairs viz. single sided patch repair and double sided patch repair. In case of single sided patch, the composite patch is applied only on one side whereas in double sided patch, patches are applied on both sides. Basically, bonded repairs are applied either as a precaution to reinforce undamaged structures or as a remedy to cracked structures so that the stress intensity factor of the crack being repaired has been significantly reduced to an appropriate level. The multiplayer nature of a bonded repair, which comprises three different layers of materials with vastly different properties, gives rise to very complicated stress states.

### 3.4 Material properties of Composite Patch

Material selection is very important aspect of the composite patch repairs. A well-designed repair can only be effective if it is strongly bonded to the parent adherend and therefore the issues of adhesive bond strength and bond durability are absolutely crucial for a fully successful repair. Generally, the material of the panel is aluminium alloy 2024-T3. The adhesive used is FM-77.
The material properties of panel, adhesive and patch are given below in Table 2.

**Table 2:** Material properties of panel, adhesive and patch [8]

| Material | $E_x$ (GPa) | $E_{y,}$ $E_z$ (GPa) | $\upsilon_{xy,}$ $\upsilon_{xz}$ | $\upsilon_{yz}$ | $G_{xy}$ $G_{xz}$ (GPa) | $G_{yz}$ (GPa) |
|---|---|---|---|---|---|---|
| Aluminium | 71.02 | | 0.3 | | | |
| Adhesive-FM77 | 1.83 | | 0.33 | | | |
| Boron/epoxy | 208.1 | 24.44 | 0.1677 | 0.035 | 7.24 | 4.94 |

There are two types of patch material viz. metallic and non-metallic. The usual objective of a Bonded Repair is to restore the damaged structure back to its original condition in terms of strength and stiffness. For this reason, perhaps the most obvious choice of metallic repair material is that which the structure is already made from. Coming to non-metallic materials, the two main non-metallic materials used are boron/epoxy and graphite/epoxy composites. Glass fibre composites are not used due to their low stiffness. The advantages of the composite material for patch is that they are light weight, corrosion and fatigue resistant, high stiffness, Easy to form strong durable bond (if thermoset), excellent formability to curved surfaces.

### 3.5 Finite Element Modeling

In this section, finite element modeling of panel repaired with single and double sided has been considered. Initially, uncracked mesh is created and then crack-blocks are inserted into it to create cracked mesh. While modeling the initial uncracked mesh, care has to be taken to make the mesh suitable according to the orientation of the crack. This is because crack blocks have to be orientated suitably to get the required initial crack.

### 3.5.1 Straight Center Crack Model

#### 3.5.1.1 Single Side Patch model

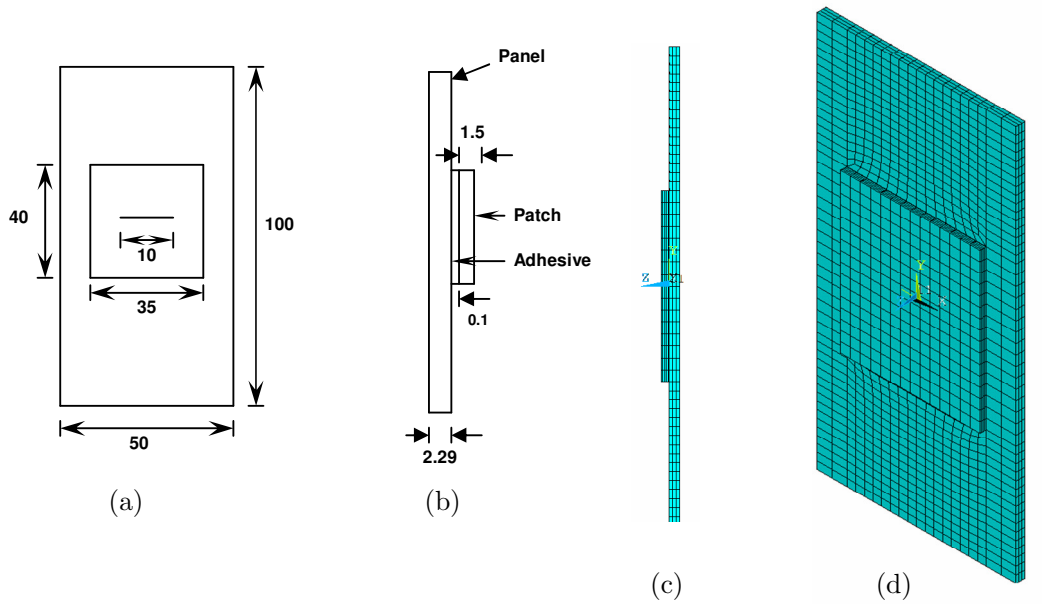


**Fig. 3.1:** (a) Front view of single patch model (b) Side view of single patch model (All dimensions are in mm) (c) Side view of meshed single patch model (d) Isometric view of meshed single patch model (e) Zoomed portion of mesh around crack tip.

Figure 3.1 shows the dimensions and finite element meshed model of the single sided patch model of straight crack model. As shown in figure, the length of patch is 40mm and width is 35mm. The dimensions of the panel are same as mentioned in previous section. The material used for panel is Aluminium-2024 T3. Material used for adhesive is FM-77 and that for patch Boron Epoxy. The fiber orientation for patch is $\vartheta = 90$. Ansys 12.1 is used for modeling. Element type used is 8-node solid element, in Ansys terminology it is SOLID185. Three elements are used along the thickness of panel. The standard type of crack block is used. Crack block used is

s02_t19x1. The lower end of the panel is fixed and is subjected to in-plane load of 118 MPa at the top end. While modeling, multipoint constraint has been used in between panel and adhesive and also in between adhesive and patch. After some crack growth, curved crack front gets generated. Curved crack front makes the analysis more tough and challenging. The analysis has been carried out by using both Paris as well as by Forman's law.

#### 3.5.1.2 Double Side Patch model

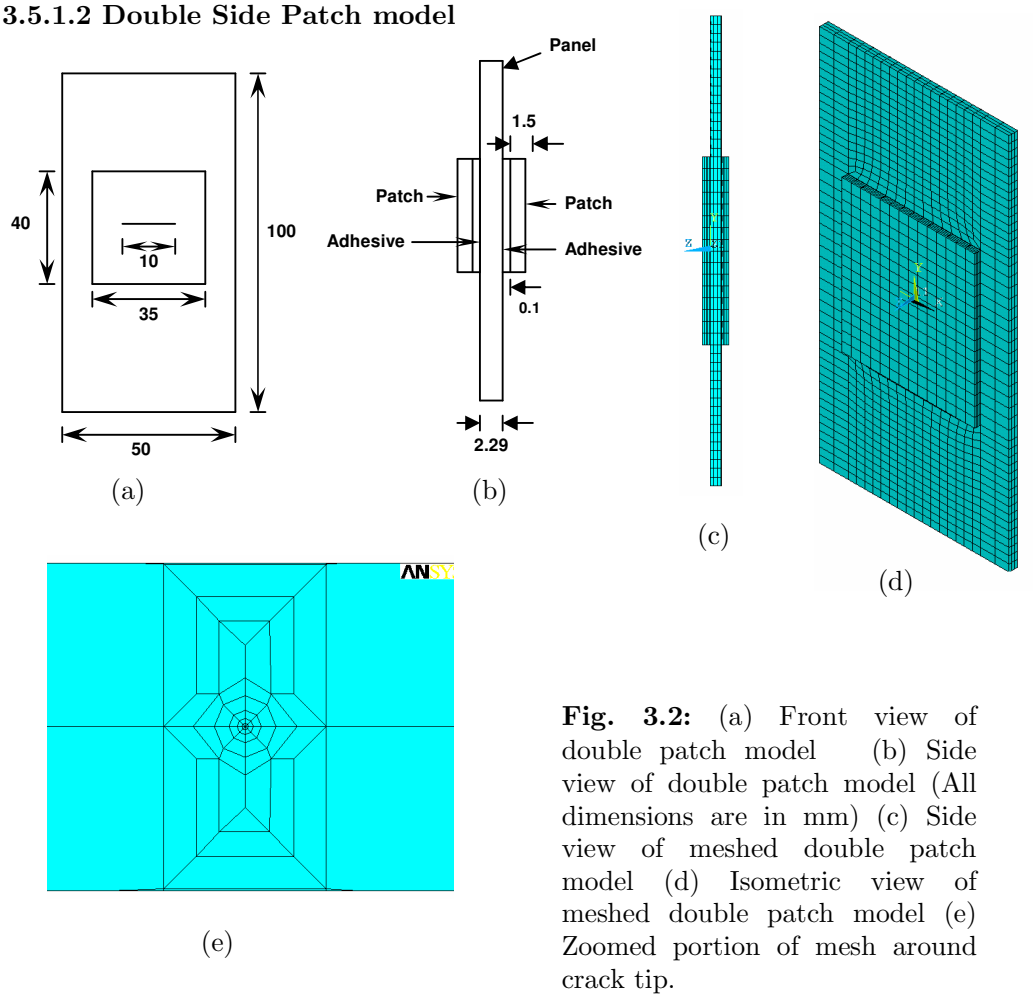


**Fig. 3.2:** (a) Front view of double patch model (b) Side view of double patch model (All dimensions are in mm) (c) Side view of meshed double patch model (d) Isometric view of meshed double patch model (e) Zoomed portion of mesh around crack tip.

Figure 3.2 shows the dimensions and finite element meshed model of the double sided patch model of straight crack model. As shown in figure, the length of patch is 40mm and width is 35mm. The dimensions of the panel are same as mentioned in previous section. The material used for panel is Aluminium-2024 T3. Material used for adhesive is FM-77 and that for patch Boron Epoxy. The fiber orientation for

patch is $\vartheta = 90$. Ansys 12.1 is used for modeling. Element type used is 8-node solid element, in Ansys terminology it is SOLID185. Three elements are used along the thickness of panel. The standard type of crack block is used. Crack block used is s02_t19x1. The lower end of the panel is fixed and is subjected to in-plane load of 118 MPa at the top end. While modeling, multipoint constraint has been used in between panel and adhesive and also in between adhesive and patch. The analysis has been carried out by using both Paris as well as by Forman's law.

### 3.5.2 Inclined Center Crack Model

The inclined crack analysis has been carried out for various crack inclination angles of 30°, 45° and 60°. The initial uncracked mesh for all the crack inclination angles is almost same. Inclined crack analysis has been carried out for unrepaired panel, single side patch and double sided patch for crack inclination angles of 30°, 45° and 60°. The analysis has been carried out for the patch with $[90_4]$ and $[90_2/0_2]$ configurations.

#### 3.5.2.1 Single Side Patch model

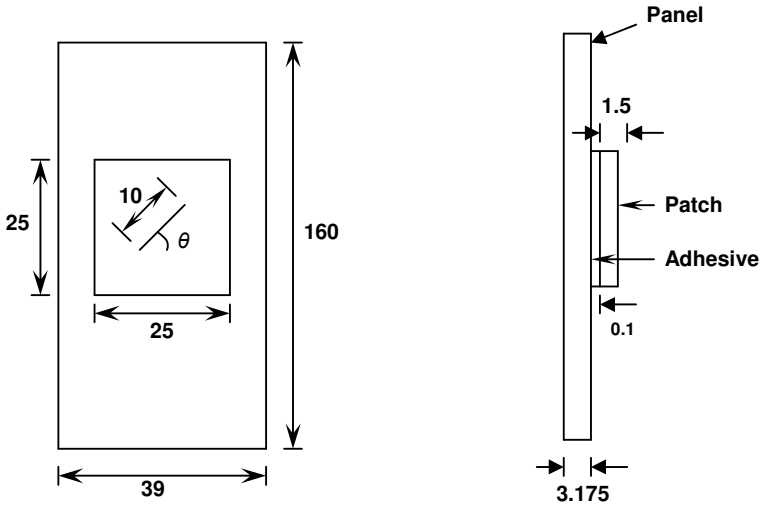


(a) (b)

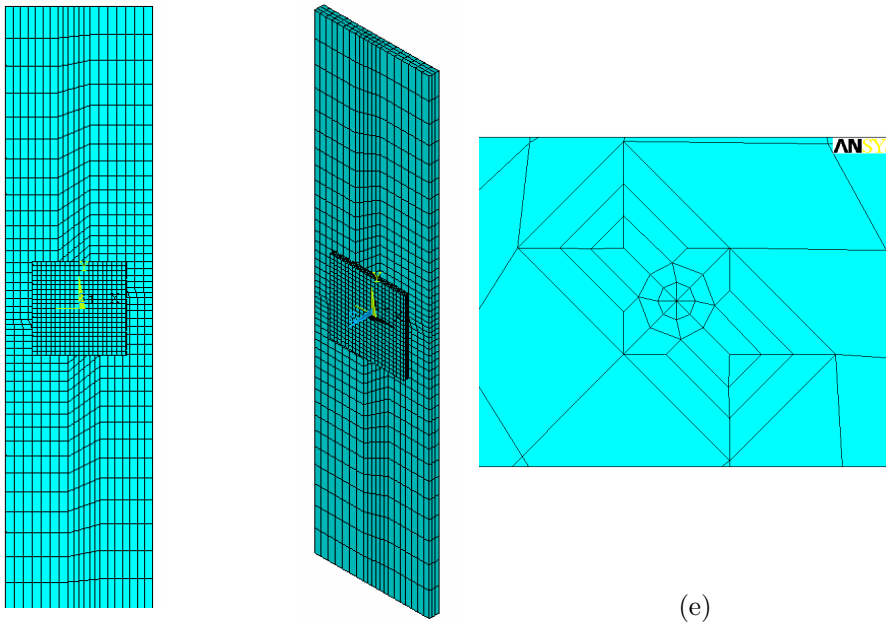


**Fig. 3.3:** (a) Front view of single patch model with inclined center crack (b) Side view of single patch model with inclined center crack (All dimensions are in mm) (c) Front view of meshed single patch model with inclined center crack (d) Isometric view of meshed single patch model with inclined center crack (e) Zoomed portion of mesh around crack tip.

The fig.3.3 above shows the dimensions of the inclined crack specimen with single sided patch. As shown in figure, its length is 160mm and width is 39mm. The patch is having length and width of 25mm. Initial crack length (2a) is 10mm. The thickness of panel is 3.175mm. Thickness of adhesive and patch is 0.1mm and 1.5mm respectively. The material used for panel is Aluminium-2024 T3. Material used for adhesive is FM-77 and that for patch Boron Epoxy. Fiber orientation for patch is $\vartheta = 90$. Ansys 12.1 is used for modeling. Element type used is 8-node solid element, in Ansys terminology it is SOLID185. Three elements are used along the thickness of panel. The standard type of crack block is used. Crack block used is s02_t19x1. The lower end of the panel is fixed and is subjected to in-plane load of 121.11 MPa at the top end. The analysis has been carried out for crack inclination angles of 30°, 45° and 60°. While modeling, multipoint constraint has been used in between panel and adhesive and also in between adhesive and patch. After some crack growth, it generates curved non-coplanar crack front. This makes the analysis

tough and challenging. The analysis has been carried out by using both Paris as well as by Forman's law.

#### 3.5.2.2 Double Side Patch model

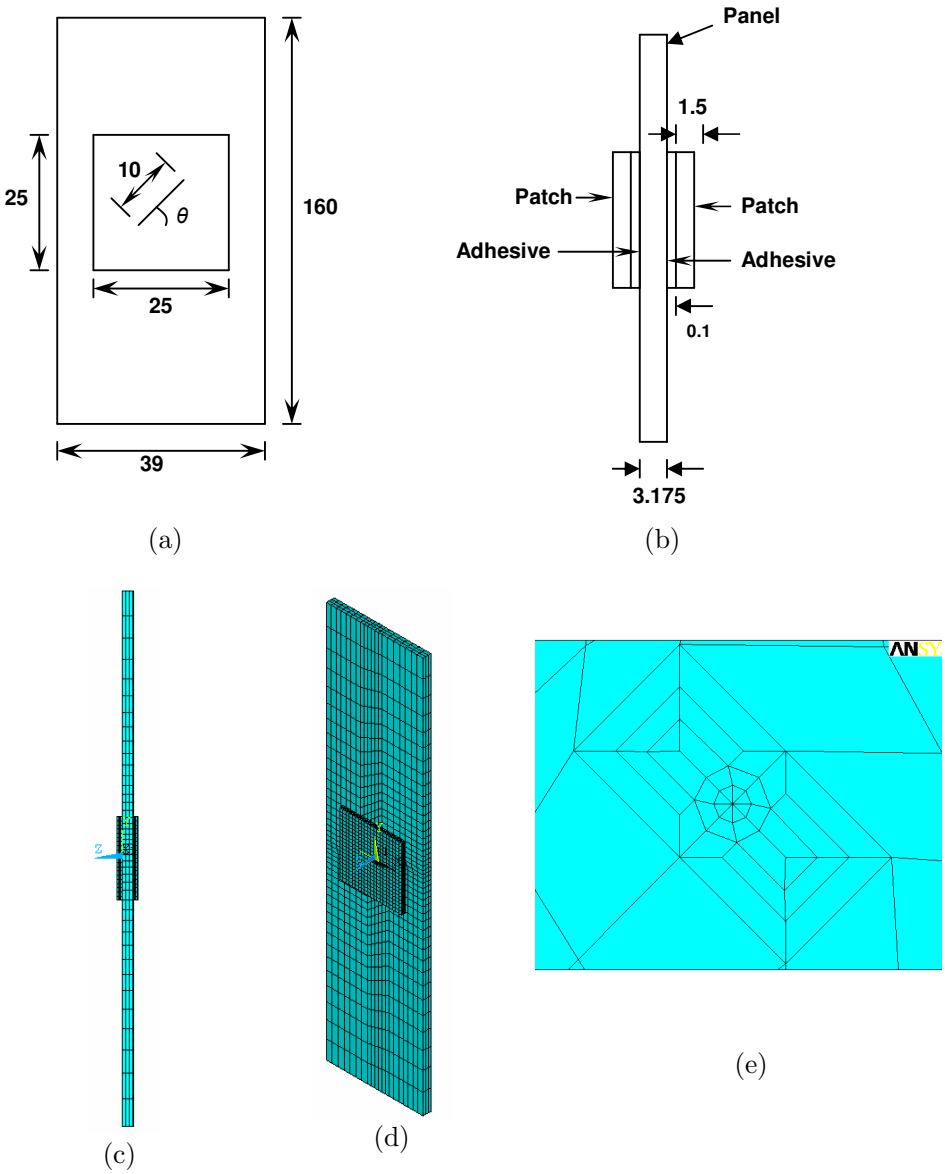


**Fig. 3.4:** (a) Front view of double patch model with inclined center crack (b) Side view of double patch model with inclined center crack (All dimensions are in mm) (c) Front view of meshed double patch model with inclined center crack (d) Isometric view of meshed double patch model with inclined center crack (e) Zoomed portion of mesh around crack tip.

The fig.3.4 above shows the dimensions of the inclined crack specimen with double sided patch. As can be seen from the figure, patches have been applied on both sides of the panel. As shown in figure, its length is 160mm and width is 39mm. The patch is having length and width of 25mm. Initial crack length (2a) is 10mm. The thickness of panel is 3.175mm. Thickness of adhesive and patch is 0.1mm and 1.5mm respectively. The material used for panel is Aluminium-2024 T3. Material used for adhesive is FM-77 and that for patch Boron Epoxy. Fiber orientation for patch is $\vartheta = 90$. Ansys 12.1 is used for modeling. Element type used is 8-node solid element, in Ansys terminology it is SOLID185. Three elements are used along the thickness of panel. The standard type of crack block is used. Crack block used is s02_t19x1. The lower end of the panel is fixed and is subjected to in-plane load of 121.11 MPa at the top end. The analysis has been carried out for crack inclination angles of 30°, 45° and 60°. While modeling, multipoint constraint has been used in between panel and adhesive and also in between adhesive and patch. The analysis has been carried out by using both Paris as well as by Forman's law.

### 3.5.3 Transversely Graded Patch Model

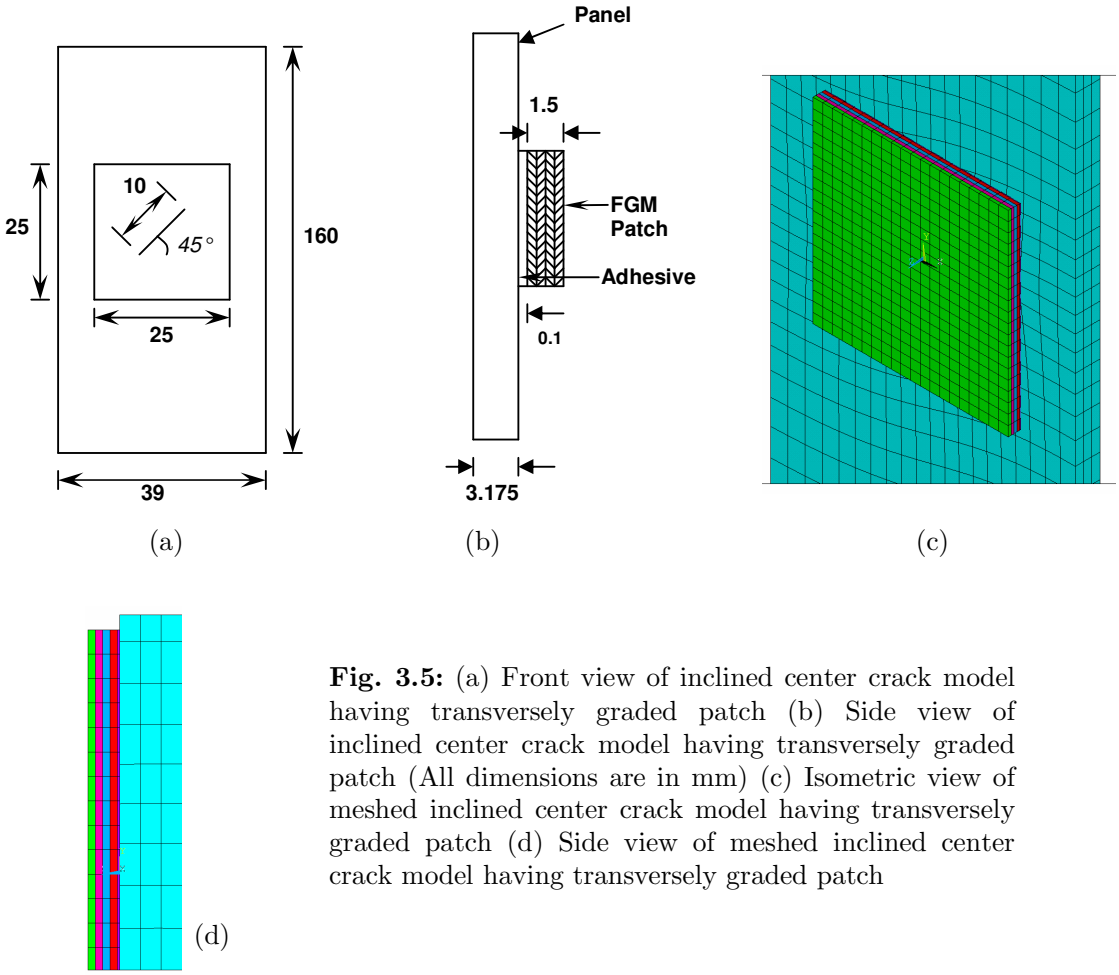


**Fig. 3.5:** (a) Front view of inclined center crack model having transversely graded patch (b) Side view of inclined center crack model having transversely graded patch (All dimensions are in mm) (c) Isometric view of meshed inclined center crack model having transversely graded patch (d) Side view of meshed inclined center crack model having transversely graded patch

The fig.3.5 above shows the dimensions of the inclined crack specimen with transversely graded patch. As shown in fig. 2.14, length of the panel is 160mm and width is 39mm. The patch is having length and width of 25mm. Initial crack length (2a) is 10mm. The thickness of panel is 3.175mm. Thickness of adhesive and patch is 0.1mm and 1.5mm respectively. The material used for panel is Aluminium-2024 T3. Material used for adhesive is FM-77. Patch is made of transversely graded material. Fiber orientation for patch is $\vartheta = 90$. The patch is having four layers. Each layer has different material properties. The material properties for different layers are shown in table 3. Ansys 12.1 is used for modeling. The variation of elastic modulus along the thickness of patch has been shown in fig. 3.6.

Table 3. Material Properties of Transversely Graded Patch

| Layer | Elasticity Modulus (GPa) | Poisson's Ratio |
|---|---|---|
| First | 206.25 | 0.3 |
| Second | 218.75 | 0.3 |
| Third | 231.25 | 0.3 |
| Fourth | 243.75 | 0.3 |

Element type used is 8-node solid element, in Ansys terminology it is SOLID185. Three elements are used along the thickness of panel. The standard type of crack block is used. Crack block used is s02_t19x1. The lower end of the panel is fixed and is subjected to in-plane load of 121.11 MPa at the top end. While modeling, multipoint constraint has been used in between panel and adhesive and also in between adhesive and patch. The analysis has been carried out by using both Paris law.

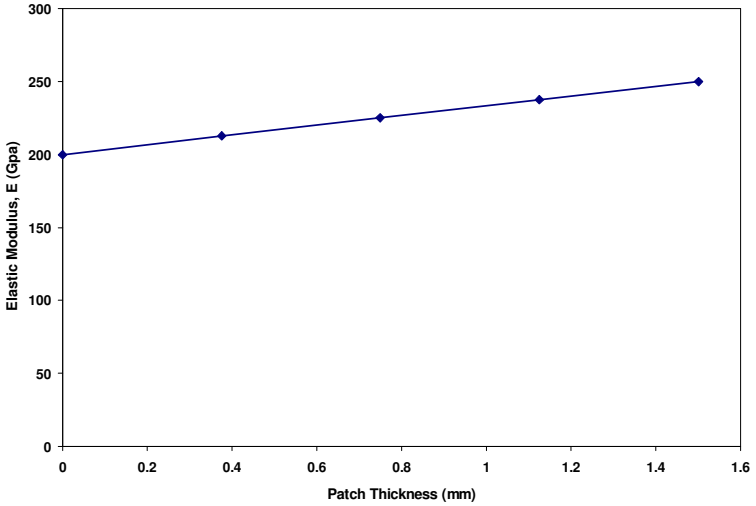


**Fig. 3.6:** Variation of Elastic Modulus, E (GPa) with Patch Thickness.

## 3.6 Results and Discussions

### 3.6.1 Validation of Results

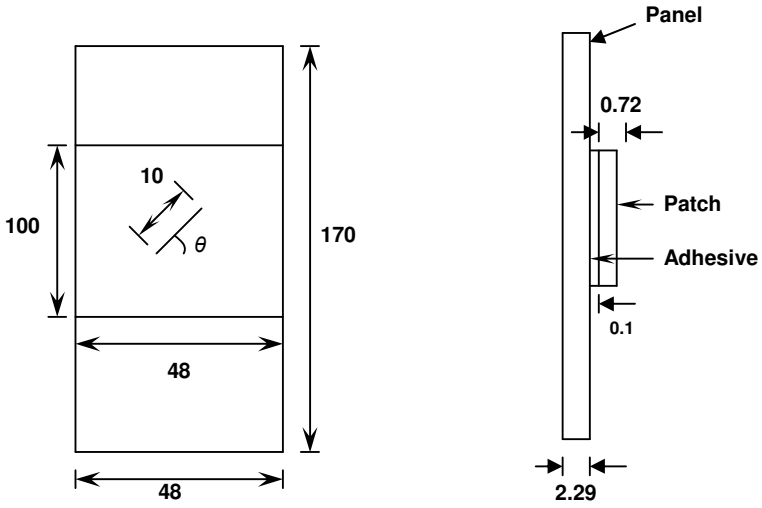


(a) (b)

**Fig. 3.7:** (a) Front view of inclined center crack model having single side patch (b) Side view of inclined center crack model having single side patch (All dimensions are in mm)

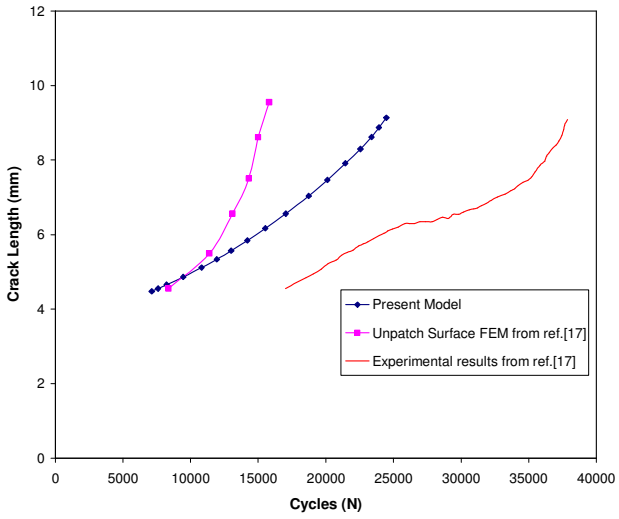


**Fig. 3.8:** Comparison of variation of sum of da with number of cycles for single side patch model from ref.[17] with experimental and unpatch surface results.

The analysis was carried out for the single side patch model as shown in fig. 3.7. The fig. 3.8 shows the comparison of the number of cycles obtained from zencrack and that from ref. [17] for single sided patch model. The number of cycles from ref. [17] for crack length of 9mm in X-direction is around 17500. The number of cycles obtained from the analysis is 23926. Little deviation was observed. It should be noted that the analysis has been carried out by considering straight crack front in ref. [17]. Whereas in this work, analysis was carried out by considering curved crack front which more real and challenging. Because of this reason, small deviation is possible. It should be noted that crack growth integration in Zencrack is generally a two-pass process to ensure that all nodes grow by the same number of cycles from one finite element analysis to the next [16]. In general the da will vary from node to node along the crack front.

### 3.6.2 Straight Center Crack Model

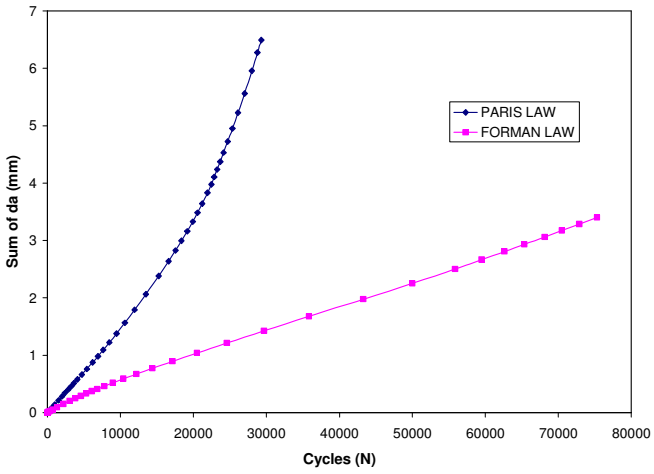


**Fig. 3.9:** Variation of Sum of da with Number of cycles (N) for single sided patch having straight center crack

Fig. 3.9 shows the variation of sum of da with number of cycles for panel repaired with single sided patch. The results are obtained for both Paris law as well as Forman law. As can be seen from the fig. 3.9, the numbers of cycles for Forman law are more. The number of cycles by using Paris law and Forman are 29299 and 75327 respectively. As can be seen from fig. 2.17 and 3.9, there is increase in number of cycles for single sided patch, thus serving the purpose of patching. Also,

we can see in fig. 3.10, life of the panel repaired with double sided patch. There is considerable increase in life of panel. For single and double sided patches, fiber orientation of $\vartheta$=90 has been used. All analyses has been carried out using curved crack front. This makes it more tough and challenging.

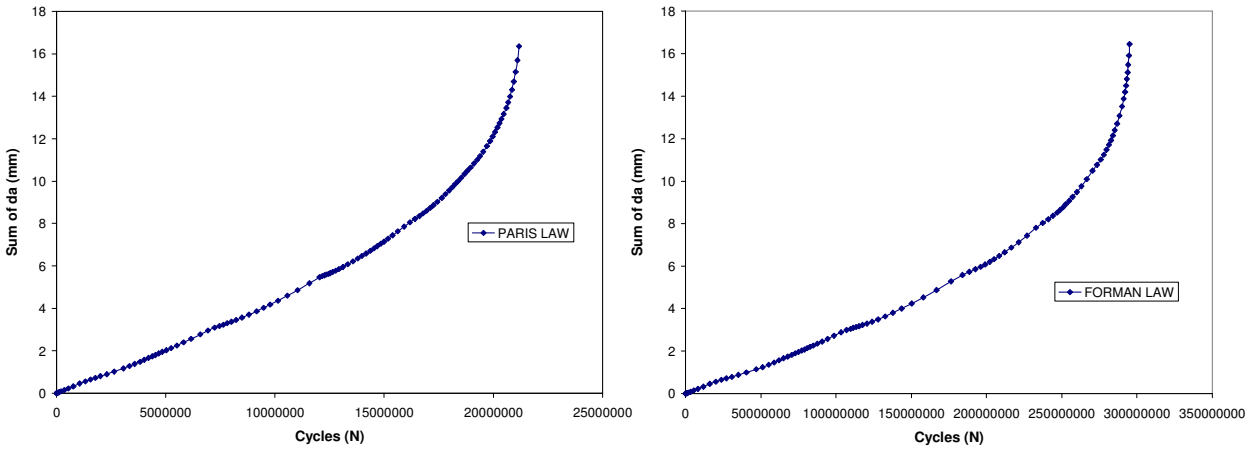


**Fig. 3.10:** (a) Variation of Sum of da with Number of cycles (N) for double sided patch having straight center crack with Paris law (b) Variation of Sum of da with Number of cycles (N) for double sided patch having straight center crack with Forman law

### 3.6.3 Inclined Center Crack Model

#### 3.6.3.1 30° Crack Inclination Angle

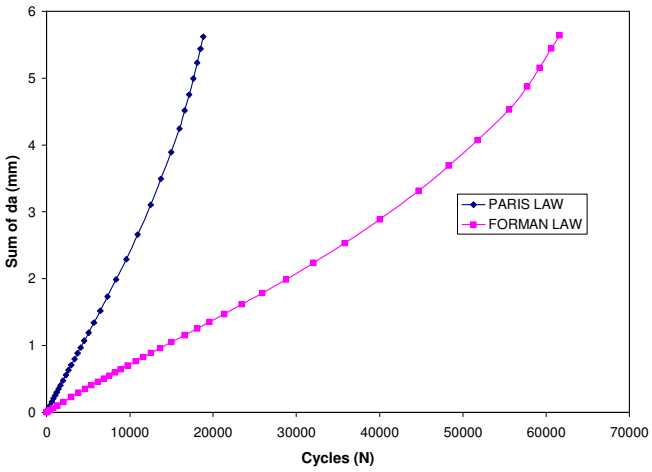


**Fig. 3.11:** Variation of Sum of da with Number of cycles (N) for single sided patch having inclined center crack with crack inclination angle of 30°

Fig. 3.11 shows the variation of sum of da with number of cycles for panel repaired with single sided patch. The results are obtained for both Paris law as well as Forman law. As can be seen from the fig. 3.11, the numbers of cycles for Forman law are more than Paris law. The number of cycles by using Paris law and Forman are 18827 and 61616 respectively. As can be seen from fig. 2.18 and 3.11, there is increase in number of cycles for single sided patch, thus serving the purpose of patching. Also, we can see in fig. 3.12, life of the panel repaired with double sided patch. There is considerable increase in life of panel. For single and double sided patches, fiber orientation of $\vartheta$=90 has been used. All analyses has been carried out using curved crack front. This makes it more tough and challenging.

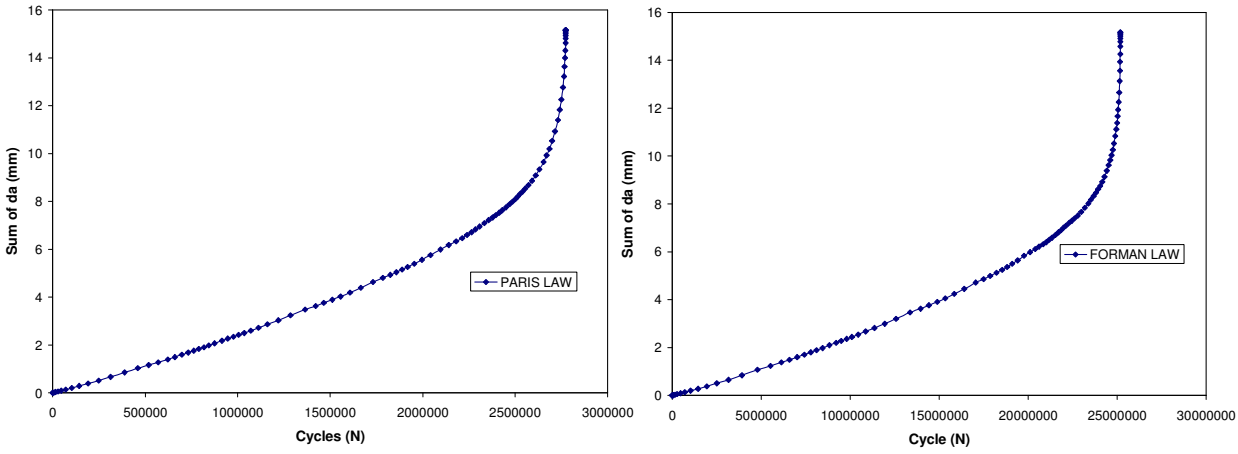


(a) (b)

**Fig. 3.12:** (a) Variation of Sum of da with Number of cycles (N) for double sided patch having inclined center crack with crack inclination angle of 30° with Paris law (b) Variation of Sum of da with Number of cycles (N) for double sided patch having inclined center crack with crack inclination angle of 30° with Forman law

#### 3.6.3.2 45° Crack Inclination Angle

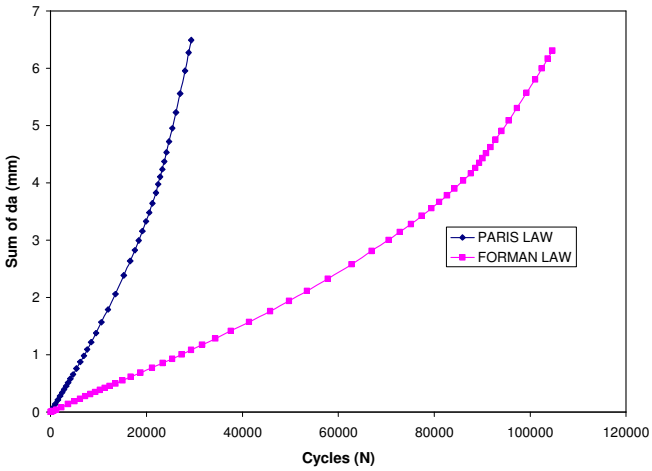


**Fig. 3.13:** Variation of Sum of da with Number of cycles (N) for single sided patch having inclined center crack with crack inclination angle of 45°

Fig. 3.13 shows the variation of sum of da with number of cycles for panel repaired with single sided patch. The results are obtained for both Paris law as well as Forman law. As can be seen from the fig. 3.13, the numbers of cycles for Forman law are more than Paris law. The number of cycles by using Paris law and Forman are 29299 and 104609 respectively. As can be seen from fig. 2.19 and 3.13, there is increase in number of cycles for single sided patch, thus serving the purpose of patching.

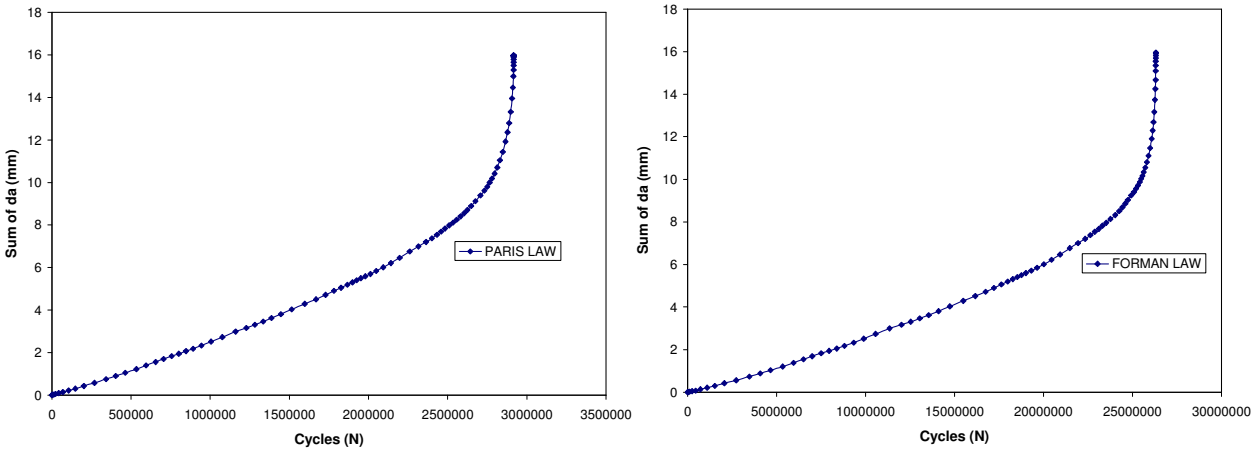


(a) (b)

**Fig. 3.14:** (a) Variation of Sum of da with Number of cycles (N) for double sided patch having crack inclination angle of 45° with Paris law (b) Variation of Sum of da with Number of cycles (N) for double sided patch with crack inclination angle of 45° with Forman law

Also, we can see in fig. 3.14, life of the panel repaired with double sided patch. There is considerable increase in life of panel. For single and double sided patches, fiber orientation of $\vartheta$=90 has been used. All analyses has been carried out using curved crack front. This makes it more tough and challenging.

#### 3.6.3.3 60° Crack Inclination Angle

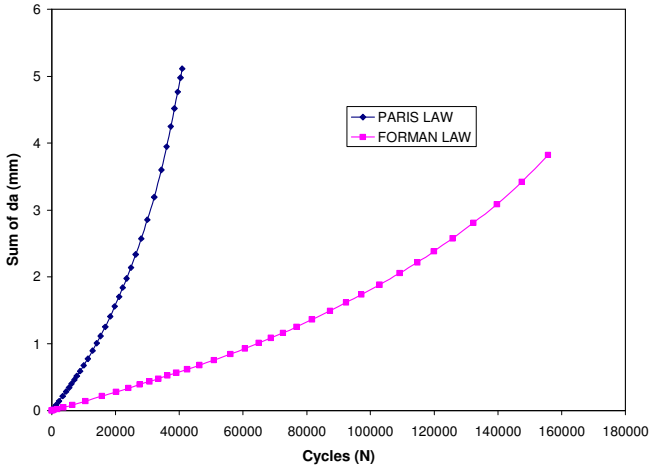


**Fig. 3.15:** Variation of Sum of da with Number of cycles (N) for single sided patch having inclined center crack with crack inclination angle of 60°

Fig. 3.15 shows the variation of sum of da with number of cycles for panel repaired with single sided patch. The results are obtained for both Paris law as well as Forman law. As can be seen from the fig. 3.15, the numbers of cycles for Forman law are more than Paris law. The number of cycles by using Paris law and Forman are 40918 and 155685 respectively.

As can be seen from fig. 2.19 and 3.15, there is increase in number of cycles for single sided patch, thus serving the purpose of patching. Also, we can see in fig. 3.16, life of the panel repaired with double sided patch. There is considerable increase in life of panel. For single and double sided patches, fiber orientation of $\vartheta$=90 has been used. All analyses have been carried out using curved crack front. This makes it more tough and challenging.

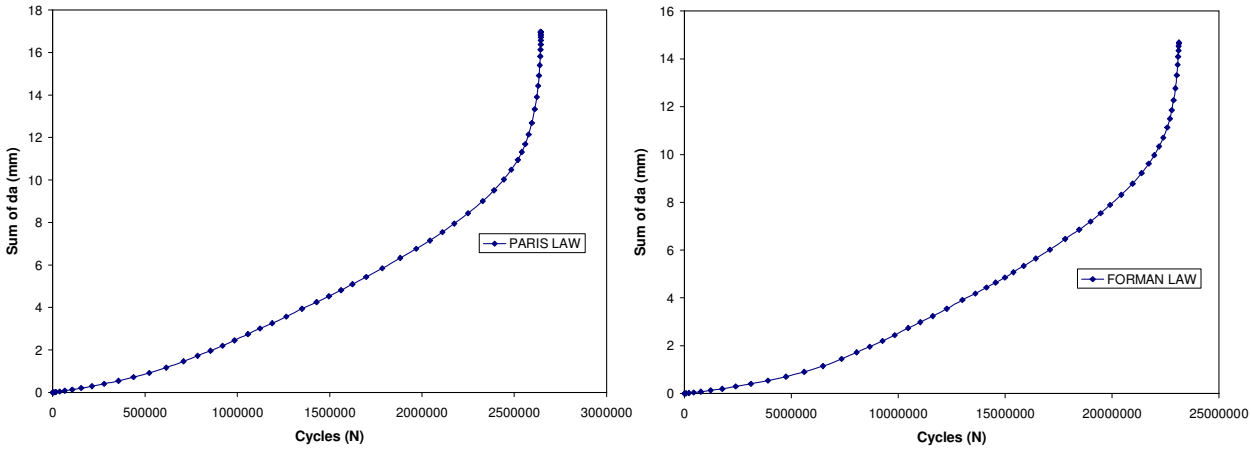


(a) (b)

**Fig. 3.16:** (a) Variation of Sum of da with Number of cycles (N) for double sided patch having inclined center crack with crack inclination angle of 60° with Paris law (b) Variation of Sum of da with Number of cycles (N) for double sided patch having inclined center crack with crack inclination angle of 60° with Forman law

### 3.6.4 Results with Unbalanced Patch model

#### 3.6.4.1 30° Crack Inclination Angle

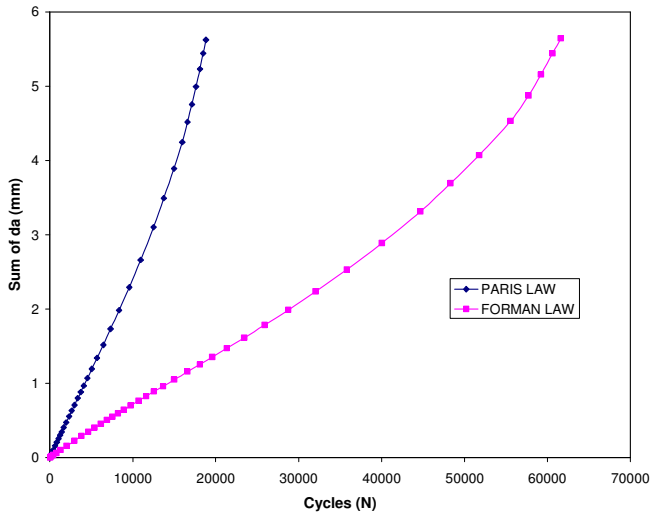


**Fig. 3.17:** Variation of Sum of da with Number of cycles (N) for unbalanced patch having inclined center crack with crack inclination angle of 30°

Fig. 3.17 shows the variation of sum of da with number of cycles for unbalanced patch for center inclined crack with crack inclination angle of 30°. For unbalanced patch, two layers in patch have fiber orientation of 90° while remaining two layers have fiber orientation of 0°. As can be seen from fig. 3.17, numbers of cycles by Forman law are more than that of Paris law. The number of cycles with Paris and Forman law is 18827 and 61616 respectively. We can see that there is hardly any difference with the $[90]_4$ configuration results.

#### 3.6.4.2 45° Crack Inclination Angle

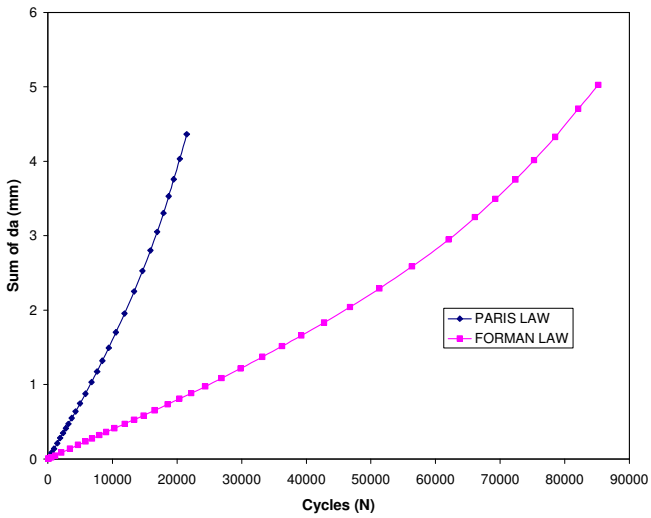


**Fig. 3.18:** Variation of Sum of da with Number of cycles (N) for unbalanced patch having inclined center crack with crack inclination angle of 45°

Fig. 3.18 shows the variation of sum of da with number of cycles for unbalanced patch for center inclined crack with crack inclination angle of 45°. For unbalanced patch, two layers in patch have fiber orientation of 90° while remaining two layers have fiber orientation of 0°. As can be seen from fig. 3.18, numbers of cycles by Forman law are more than that of Paris law. The number of cycles with Paris and Forman law is 21472 and 85198 respectively.

#### 3.6.4.2 60° Crack Inclination Angle

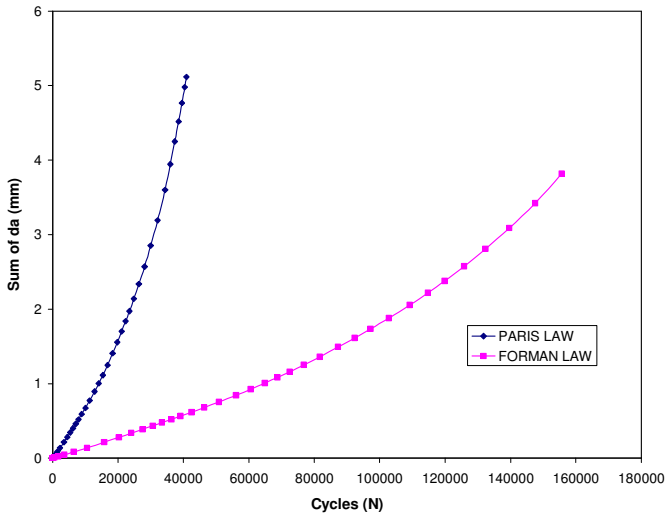


**Fig. 3.19:** Variation of Sum of da with Number of cycles (N) for unbalanced patch having inclined center crack with crack inclination angle of 60°

Fig. 3.19 shows the variation of sum of da with number of cycles for unbalanced patch for center inclined crack with crack inclination angle of 60°. For unbalanced patch, two layers in patch have fiber orientation of 90° while remaining two layers have fiber orientation of 0°. As can be seen from fig. 3.19, numbers of cycles by Forman law are more than that of Paris law. The number of cycles with Paris and Forman law is 40918 and 155685 respectively. We can see that there is hardly any difference with the $[90]_4$ configuration results.

### 3.6.5 Result with Transversely Graded Patch model

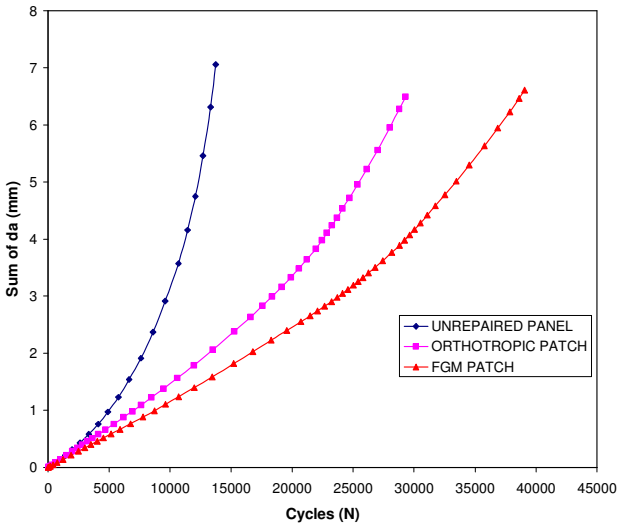


**Fig. 3.20:** Variation of Sum of da with Number of cycles (N) for inclined center crack with crack inclination angle of 45° having transversely graded patch

Above fig. 3.20 shows the variation of sum of da with number of cycles for inclined center crack with crack inclination angle of 45° having transversely graded patch. It can be seen that number of cycles are 39058. We can see from fig. 3.13 and 3.20 that for the same unrepaired panel, number of cycles with transversely graded patch is more. Hence, it is advantageous to use transversely graded patch rather than usual $[90]_4$ orthotropic patch. The details of the modeling and material properties of transversely graded patch are already discussed in section 2.3.3.5.3.

## 3.7 Crack Growth Profiles

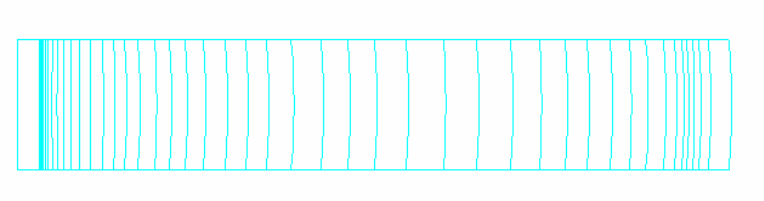

**Fig. 3.21:** Crack growth profile through thickness of unrepaired inclined crack panel

Above Fig. 3.21 shows the crack growth profile through thickness of the unrepaired panel. It can be seen from the figure that the crack front shape is curved.

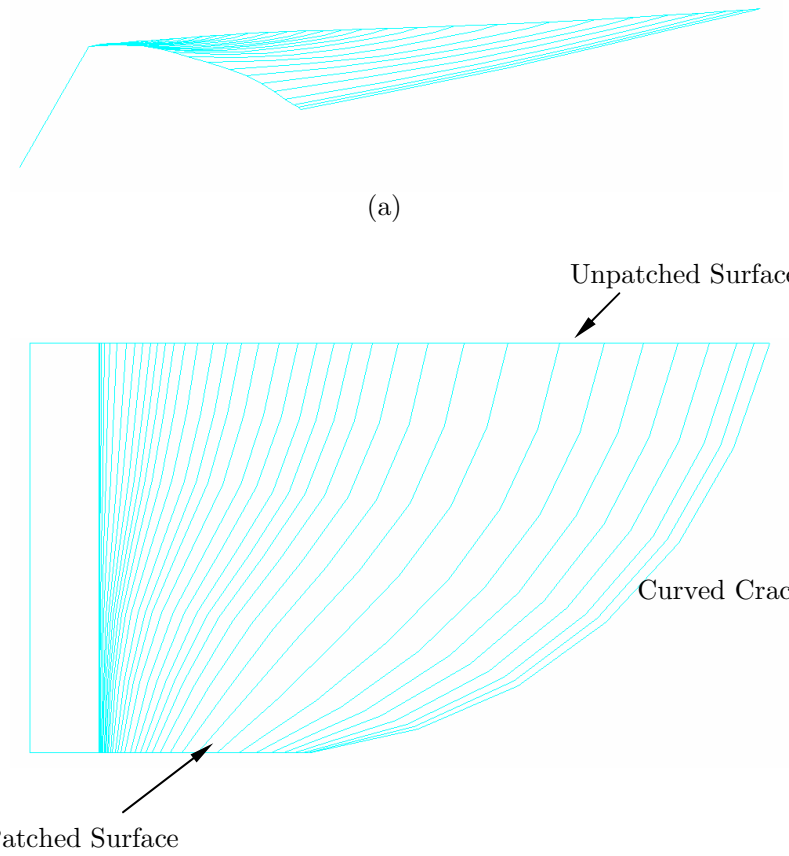


(a)

(b)

**Fig. 3.22:** (a) Front view of the crack growth profile of inclined crack panel repaired with single sided patch (b) Top view of the crack growth profile through thickness of inclined crack panel repaired with single sided patch

Fig. 3.22 shows the crack growth profiles of the inclined crack panel repaired with single sided patch. It can be seen that the crackfront shape is curved. It can be seen that crack grows at faster rate on unpatched surface than on the patched surface. This gives rise to the curved crackfront. It can be seen from fig. 3.22 (a) that the crackfront is non-planar also. So, crackfront shape is non-planar and curved. This makes the analysis challenging. Because of this, lots of problems have to be faced during modeling and in initial mesh pattern. The crackfront shape of double sided patch is similar to fig. 3.21.

## 3.8 Closure

Three dimensional analysis has been carried out for straight and inclined center crack specimens. Three dimensional analysis is carried out by considering curved crack front shape. This makes it more challenging and tough, especially for single sided patch. During crack propagation in single sided patch in mixed mode condition, it develops the curved and non planar crack front. Also because of the shift in neutral axis, bending is involved. This makes it most challenging. All the analyses have been carried out using both Paris law and Forman law. It can be seen that the number of cycles for inclined crack increases as initial crack inclination angle increases. The numbers of cycles are more for the 60° than that for 45° and 30°. It can be seen that there is there is considerable increase in life of panel after patching.

For single sided patches, increase in life of the panel is around 60-70%. For unbalanced patches, the number of cycles is almost same as those with $[90]_4$ patch configuration. Not much difference has been observed in the results with unbalanced patches.

For transversely graded patch, it has been observed that number of cycles are more than orthotropic patch. Hence, it is advantageous to use functionally graded patch than orthotropic patch.

# Chapter 4

# Recommendations for Future Work

In this work, two-dimensional and three-dimensional fatigue crack propagation analysis was carried out for mode I and mixed mode conditions. Two-dimensional analysis was carried out for edge crack specimens in both mode I and mixed mode conditions. It was observed that life increases with reduction in crack inclination angle. Three-dimensional analysis was carried out for unrepaired panel and for panel repaired with single and double side composite patches. During the three-dimensional analysis, non uniform crack growth (NUCG) which results in curved crack front has been considered. This makes the analysis tough and challenging especially for single side patch. Analysis was carried out using Paris law and Forman law. It has been shown that the life of the panel increases after patching. The effect of initial crack inclination angle has also been studied. It was observed that life of the panel increases as the crack inclination angle increases. Study has also been carried out with unbalanced patch. For unbalanced patches, the number of cycles is almost same as those with $[90]_4$ patch configuration. Not much difference has been observed in the results with unbalanced patches. The analysis was carried out with transversely graded patch. For transversely graded patch, it has been observed that numbers of cycles are more than orthotropic patch. Hence, it is advantageous to use transversely graded patch than orthotropic patch for higher fatigue life.

In case of single sided patch under mixed mode condition, crack front develops into a curved and non-planar (skewed) crack front with time. This causes the severe

distortions in the elements of crack block and elements surrounding it. Hence, an adaptive meshing needs to be evolved for handling such behaviours.

Also a very high mesh density has been utilised in the present study and it severely increases the computational time for analysis. A systematic study needs to be done for building a model with an optimum mesh density without compromising on the accuracy of the results.

As the SIF is varying across the thickness of the panel therefore fatigue life estimation depends on how you choose the SIF values. One can take average of it across the thickness otherwise the highest value. A suitable model needs to be predicted on these lines for accurate life estimation.

The analysis has been carried out for the $[90]_4$ fiber orientation. In future, analysis can be carried out for different patch layup such as $[105]_4$, $[-45]_4$, $[-45/+45]_2$ in order to study the effect of fiber orientation on fatigue life.

In this study only linear fracture mechanics is considered but in practice fatigue crack growth is associated with non-linear fracture mechanics where plastic effect is considered around the crack tip. Also certain phenomenons like crack closure and overload needs to be studied for the repaired panels under fatigue load.

# Appendix A

# Details of Zencrack Commands

As mentioned in earlier section 3.4, for carrying out analysis we need two files namely "Uncracked mesh file" having ".ans" as its extension and "Zencrack command file" having ".zcr" as its extension, commonly called "zcr file". These two files need to be kept in same folder. Before running the Zencrack command file, change the folder by using "cd" command in the Zencrack command window. Now, we will discuss the details of Zencrack command file.

Now, let us take example of both the files. The typical "Uncracked file" will look as below. It is for creating panel for straight center crack [Ref. Fig. 2.8]

```
/COM,  Structural
! Entering Preprocessor
/PREP7
ET,1,185
k,1,17.5,20
k,2,-17.5,20
k,3,-17.5,-20
k,4,17.5,-20
k,5,17.5,20
k,6,-17.5,20
k,7,-17.5,-20
k,8,17.5,-20
k,9,25,50
k,10,-25,50
k,11,-25,-50
k,12,25,-50
K,13,17.5,20,0.1
K,14,-17.5,20,0.1
K,15,-17.5,-20,0.1
K,16,17.5,-20,0.1
K,17,25,20
K,18,-25,20
K,19,-25,-20
K,20,25,-20
K,21,17.5,50
```

```
K,22,-17.5,50
K,23,-17.5,-50
K,24,17.5,-50
k,25,17.5,20,-2.29
k,26,-17.5,20,-2.29
k,27,-17.5,-20,-2.29
k,28,17.5,-20,-2.29
K,29,17.5,20,-2.39
K,30,-17.5,20,-2.39
K,31,-17.5,-20,-2.39
K,32,17.5,-20,-2.39

!AREAS
A,1,2,3,4 !A1
A,5,6,7,8  !A2
A,13,14,15,16  !A3
A,5,8,20,17  !A4
A,6,7,19,18  !A5
A,6,22,10,18  !A6
A,6,22,21,5   !A7
A,5,21,9,17   !A8
A,7,19,11,23   !A9
A,7,23,24,8  !A10
A,8,24,12,20  !A11
A,25,26,27,28  !A12
A,29,30,31,32  !A13
ALLSEL,ALL
ASEL,U,AREA,,1
ASEL,U,AREA,,3
ASEL,U,AREA,,12
ASEL,U,AREA,,13
APLOT
VEXT,ALL, , ,0,0,-2.29,,,,
ALLSEL,ALL
!GIVING LINESET DIVISIONS
LSEL,R,LOC,Z,0,-2.29
LSEL,U,LOC,Z,0
LSEL,U,LOC,Z,-2.29
LESIZE,ALL, , ,3, , , , ,0
ALLSEL,ALL
GPLOT
LSEL,R,LOC,Y,20
LSEL,R,LOC,X,-17.5,17.5
LSEL,U,LOC,X,-17.5
LSEL,U,LOC,X,17.5
LESIZE,ALL, , ,14, , , , ,0
ALLSEL,ALL
LSEL,R,LOC,Y,-20
LSEL,R,LOC,X,-17.5,17.5
LSEL,U,LOC,X,-17.5
LSEL,U,LOC,X,17.5
LESIZE,ALL, , ,14, , , , ,0
ALLSEL,ALL
LSEL,R,LOC,Y,20
LSEL,R,LOC,X,17.5,25
LSEL,U,LOC,X,17.5
LSEL,U,LOC,X,25
LESIZE,ALL, , ,2, , , , ,0
```

```
ALLSEL,ALL
LSEL,R,LOC,Y,20
LSEL,R,LOC,X,-17.5,-25
LSEL,U,LOC,X,-17.5
LSEL,U,LOC,X,-25
LESIZE,ALL, , ,2, , , , ,0
ALLSEL,ALL
LSEL,R,LOC,Y,-20
LSEL,R,LOC,X,17.5,25
LSEL,U,LOC,X,17.5
LSEL,U,LOC,X,25
LESIZE,ALL, , ,2, , , , ,0
ALLSEL,ALL
LSEL,R,LOC,Y,-20
LSEL,R,LOC,X,-17.5,-25
LSEL,U,LOC,X,-17.5
LSEL,U,LOC,X,-25
LESIZE,ALL, , ,2, , , , ,0
ALLSEL,ALL
LSEL,R,LOC,Y,50
LSEL,R,LOC,X,17.5,25
LSEL,U,LOC,X,17.5
LSEL,U,LOC,X,25
LESIZE,ALL, , ,2, , , , ,0
ALLSEL,ALL
LSEL,R,LOC,Y,50
LSEL,R,LOC,X,-17.5,-25
LSEL,U,LOC,X,-17.5
LSEL,U,LOC,X,-25
LESIZE,ALL, , ,2, , , , ,0
ALLSEL,ALL
LSEL,R,LOC,Y,-50
LSEL,R,LOC,X,17.5,25
LSEL,U,LOC,X,17.5
LSEL,U,LOC,X,25
LESIZE,ALL, , ,2, , , , ,0
ALLSEL,ALL
LSEL,R,LOC,Y,-50
LSEL,R,LOC,X,-17.5,-25
LSEL,U,LOC,X,-17.5
LSEL,U,LOC,X,-25
LESIZE,ALL, , ,2, , , , ,0
ALLSEL,ALL
LSEL,R,LOC,Y,50
LSEL,R,LOC,X,-17.5,17.5
LSEL,U,LOC,X,-17.5
LSEL,U,LOC,X,17.5
LESIZE,ALL, , ,16, , , , ,0
ALLSEL,ALL
LSEL,R,LOC,Y,-50
LSEL,R,LOC,X,-17.5,17.5
LSEL,U,LOC,X,-17.5
LSEL,U,LOC,X,17.5
LESIZE,ALL, , ,16, , , , ,0
ALLSEL,ALL
LSEL,R,LOC,X,17.5
LSEL,U,LOC,Y,20
LSEL,U,LOC,Y,50
```

```
LSEL,U,LOC,Y,-20
LSEL,U,LOC,Y,-50
LESIZE,ALL, , ,16, , , , ,0
ALLSEL,ALL
LSEL,R,LOC,X,-17.5
LSEL,U,LOC,Y,20
LSEL,U,LOC,Y,50
LSEL,U,LOC,Y,-20
LSEL,U,LOC,Y,-50
LESIZE,ALL, , ,16, , , , ,0
ALLSEL,ALL
LSEL,R,LOC,X,25
LSEL,U,LOC,Y,20
LSEL,U,LOC,Y,50
LSEL,U,LOC,Y,-20
LSEL,U,LOC,Y,-50
LESIZE,ALL, , ,16, , , , ,0
ALLSEL,ALL
LSEL,R,LOC,X,-25
LSEL,U,LOC,Y,20
LSEL,U,LOC,Y,50
LSEL,U,LOC,Y,-20
LSEL,U,LOC,Y,-50
LESIZE,ALL, , ,16, , , , ,0
ALLSEL,ALL
GPLOT
VMESH,ALL,,,1
SHPP,WARN
ALLSEL,ALL
nsle
cm,panel,elem

!APPLYING MATERIAL PROPERTIES OF PANEL
mp,ex,1,71020
mp,nuxy,1,0.3
ALLSEL,ALL
EPLOT


!APPLYING DOF AT BOTTOM END
ALLSEL,ALL
NSEL,R,LOC,Y,-50
D,ALL, ,0, , , ,ALL, , , , ,
ALLSEL,ALL

!APPLYING LOADS AT UPPER END
NSEL,R,LOC,Y,50
SF,ALL,PRES,-118
ALLSEL,ALL
EPLOT
FINISH

/SOLU
SOLVE
FINISH
/EXIT,SOLU
```

Typical Zencrack command file for above file will be like shown below [Ref. Fig. 2.8]:

```
*FILES,UNCRACKED=Panel.ans
*OPTIONS,FE=FULL,TYPE=FATIGUE
*CRACK FRONT, INITIAL=SIZE
s02_t19x1
72 128 113 0 0
s02_t19x1
296 821 819 0 0
s02_t19x1
520 822 820 0 0
s02_t19x1
73 821 819 0 0
s02_t19x1
297 822 820 0 0
s02_t19x1
521 383 368 0 0
*CRACK FRONT, INITIAL=SIZE
s02_t19x1
153 188 203 0 0
s02_t19x1
377 829 831 0 0
s02_t19x1
601 830 832 0 0
s02_t19x1
152 829 831 0 0
s02_t19x1
376 830 832 0 0
s02_t19x1
600 443 458 0 0
*SPLIT
136 137
360 361
584 585
120 121
344 345
568 569
*SPLIT
104 105
328 329
552 553
88 89
312 313
536 537
*LOAD SYSTEM,TYPE=CONSTANT AMPLITUDE,SCALE=1
  0.00000E+00  1.00000E+00
*CRACK GROWTH DATA,TYPE=PARIS,CONVERSION=1.00000
3.63E-13 3.2828
*MATERIAL
71020,0.3
*SAVE,DB=YES
*SAVE,RST=YES
*BOUNDARY SHIFT,TYPE=TRANSFER,SHIFT HEIGHT=YES,SURROUND FIX=YES
*RELAX
*END
```

Now, we will consider meaning of each command step by step.

i. *FILE command is used to specify the Uncracked mesh file name. Enter the name of the uncracked mesh over there. In the example considered above, "Panel" is the name of uncracked mesh file having ".ans" as its extension.

ii. *OPTIONS command is used to specify the type of analysis to be performed. In above example, keyword FE = Full is used to run full finite element analysis while keyword TYPE = Fatigue is used to carry out crack growth prediction.

iii. *CRACK FRONT command defines the crack-blocks and their position in the mesh. It also defines initial size of the crack front section within each crack block. This keyword is mandatory for all analyses. Each distinct crack front in a model must be defined using a new occurrence of this keyword and so all crack-blocks on a crack front must be listed under same keyword. In above example, there are two crack fronts. Hence, *CRACK FRONT command has been used two times. Crack front numbers are allocated sequentially by Zencrack based on the order of the *CRACK FRONT keyword(s).

iv. s02_t19X1 indicates the type of crack block used. It is standard type of crack block having deep crack and crack block transfer capability. For first crack block, number 72 indicates the element in uncracked mesh model which is to be replaced by corresponding crack block. Numbers 128 and 113 indicates corresponding node numbers to orient the crack block in required fashion. Next two 0s indicate the distance of crack tip from the edge of the element in crack block.

v. *SPLIT keyword defines the element pairs that are to be split to form a "deep" crack front. This option is to be used once for each set of elements pairs that form a set of split elements related to a crack front.

vi. *LOAD SYSTEM keyword is used to define type of loading.

vii. *CRACK GROWTH DATA is used to define crack growth data for growth prediction analysis.

viii. *MATERIAL allows the specification of material properties. In above example Young's modulus is 71020 MPa and Poisson's ratio is 0.3.

ix. *SAVE keyword allows to save the output files from Ansys. In above example, database file (DB) and results file (RST) is saved.

x. *BOUNDARY SHIFT keyword defines use of boundary shifting options.

xi. *RELAX keyword allows relaxation of the cracked finite element mesh to minimize element distortion during analysis. If this keyword is omitted then relaxation is not used.

xii. *END keyword is mandatory for all analyses and it indicates the end of input file. Any data in the input file after this keyword is ignored.

This was the step by step description of each command of zcr file.

# References


[1] Baker A. A. and Jones R., *Bonded repair of aircraft structures.* Dordrecht, Netherlands, Martinus Nijhoff Publisher, 1988.

[2] Ratwani M. M., Analysis of cracked adhesively bonded laminated structures. AIAA J, 17(4):988–94, 1979.

[3] Rose LRF. "A cracked plate repaired by bonded reinforcements" Int J Fract, 18(2):135–44, 1982.

[4] Lu L, Hu Y, Ju D. "An assessing method of fatigue life on central throughcracked plate with adhesive bounded reinforcement" Fatigue Fract Risk ASME, 215:135–40, 1991.

[5] Hosseini-Toudeshky H, Shahverdi H, Daghyani HR. "Fatigue life assessment of repaired panels with adhesively bounded composite plates." In: Second Asian–Australian conference on composite materials, ACCM-2000, Kyonju, Korea, 18–20 August, 2000.

[6] Bachir Bouiadjra B, Belhouari M, Serier B. "Computation of the stress intensity factors for repaired cracks with bonded composite patch in mode I and mixed mode.", Composite Structures, 56:401–6, 2002.

[7] Chung HK, Yang WH. Mixed-Mode fatigue crack growth in aluminium plates with composite patches. Int J Fatigue, 25:325–33, 2003.

[8] Hossein Hosseini-Toudeshky, Bijan Mohammadi and Hamid Reza Daghyani, "Mixed-mode fracture analysis of aluminium repaired panels using composite patches", Composites Science and Technology, 66:188-198, 2006.

[9] H. Hosseini-Toudeshky, "Effects of composite patches on fatigue crack propagation of single-side repaired aluminum panels", Composite Structures, 76:243–251, 2006.

[10] H. Hosseini-Toudeshky , B. Mohammadi, "A simple method to calculate the crack growth life of adhesively repaired aluminum panels", Composite Structures, 79:234–241, 2007.

[11] H. Hosseini-Toudeshky, M. Saber and B. Mohammadi, "Finite element crack propagation of adhesively bonded repaired panels in general mixed-mode conditions", Finite Elements in Analysis and Design, 45:94 -103, 2009.

[12] T.L. Anderson, Fracture Mechanics Fundamentals and Applications, 3rd edition, CRC Press, 2005.

[13] Prashant Kumar, Elements of Fracture Mechanics, Tata McGraw Hill Publishing Co. Ltd, New Delhi, 2009.

[14] Cong N. Duong and Chun Hui Wang, Composite Repair Theory and Design, Elsevier, Netherlands, 2007.

[15] Ansys version 12.1, User's Documentation, Pennsylvania, U.S, 2009.

[16] Zencrack 7.6 User's Manual, London, U.K., 2009.

[17] H. Hosseini-Toudeshky, B. Mohammadi, S. Bakhshandeh, "Mixed-mode fatigue crack growth of thin aluminium panels with single side repair using experimental and numerical methods", Fatigue Fract Engng Mater Struct, 30:629–639, 2007.

[18] Hellen TK, "On the method of virtual crack extensions", Int J Numer Meth Engng, 9: 187-207, 1975.

# List of the papers submitted on the basis of this thesis

1. M.Ramji and Amit Shankar Kulkarni, "Fatigue Crack Propagation by using Finite Element Method", Proc. International Conference on Theoretical, Applied, Computational, Experimental Mechanics 2010, IIT Kharagpur, $27^{th}$ – $29^{th}$ December, 2010.